

# SMEFT effects on gravitational wave spectrum from electroweak phase transition

---

Katsuya Hashino (Tokyo University of Science)

Collaborators: Daiki Ueda<sup>1</sup> ( 1. Peking University)

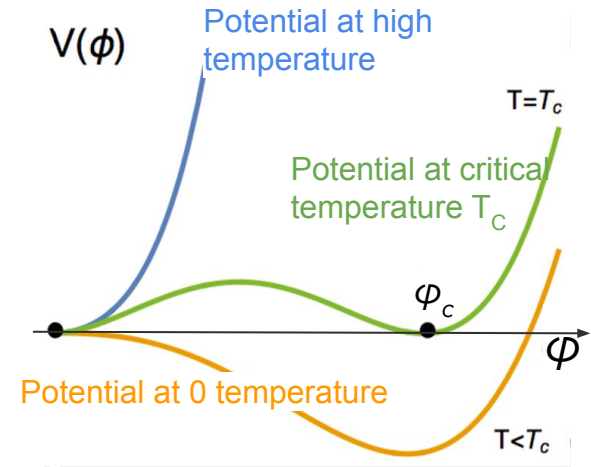
[K. H., Daiki Ueda, arXiv: 2210.11241[hep-ph] ]

# Introduction

- ★ The shape of Higgs potential is still undetermined.
  - The new physics (NP) effects can contribute to the potential.
- ★ The dynamics of electroweak phase transition (EWPT) is governed by the shape of the Higgs potential.

The EWPT in the SM is crossover.

[Y. Aoki, F. Csikor, Z. Fodor and A. Ukawa, Phys. Rev. D 60, 013001 (1999)]



**Strongly first-order EWPT can be realized by NP effects beyond the SM.**

$$(\phi_c / T_c > 1)$$

# Introduction

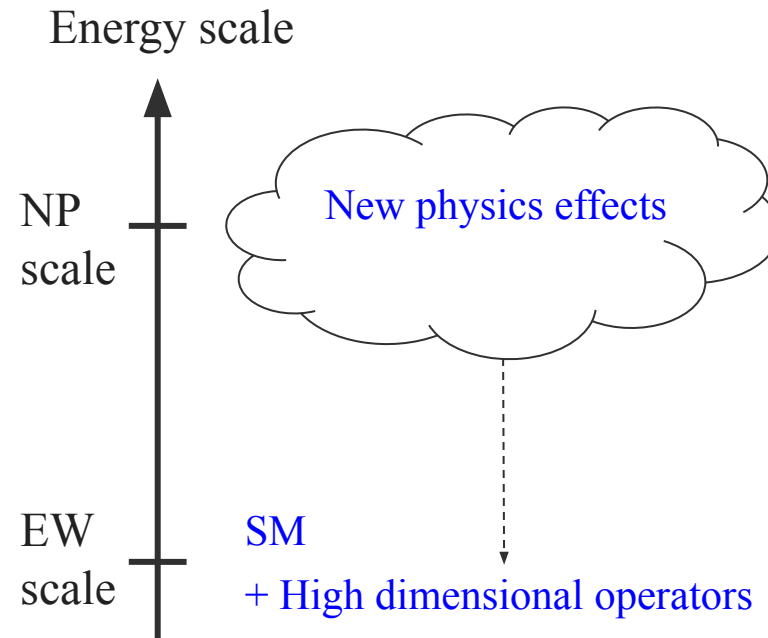
- ★ However, new particles have not been found by the Large Hadron Collider (LHC) since the discovery of the Higgs boson...

**The NP scale may be larger than the electroweak (EW) scale**



**Standard Model Effective Field Theory (SMEFT)**

In this talk, we consider this framework.



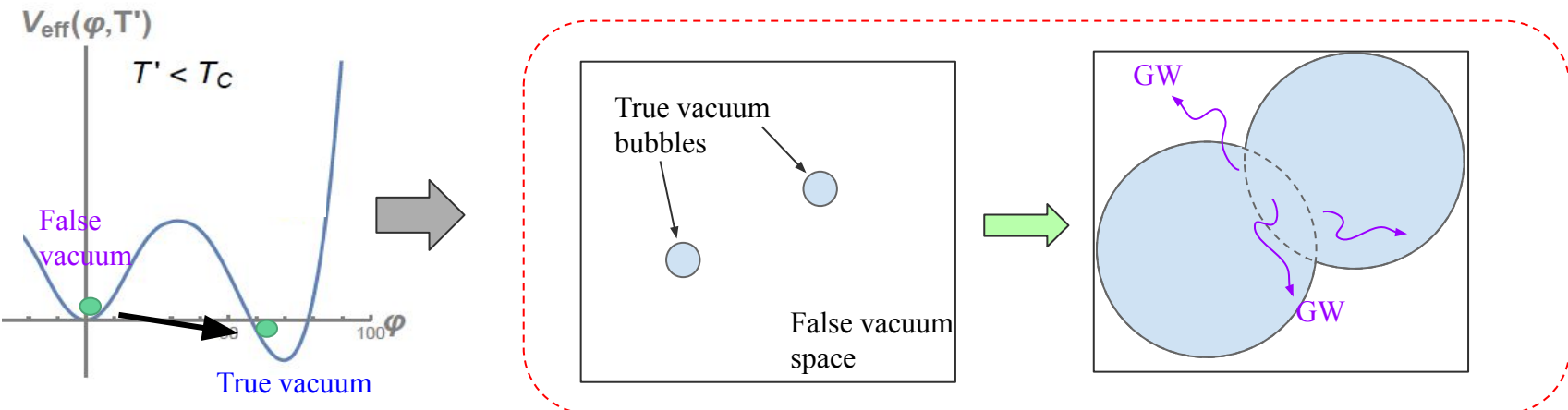
# Introduction

- ★ If the first-order phase transition occurs in the early Universe, the gravitational waves (GWs) are produced by collision of bubbles from the phase transition.

Decay rate of vacuum  $\Gamma \sim \exp\left[-\frac{16\pi S_1^3}{3T\epsilon^2}\right]$  corresponds to the critical bubble nucleation rate per unit volume and per unit time.

[L. D. Landau, E. M. Lifshitz, "Statistical Physics"]

[S. Coleman , "The uses of instantons", (1977)]



The GW spectrum depends on the potential form.

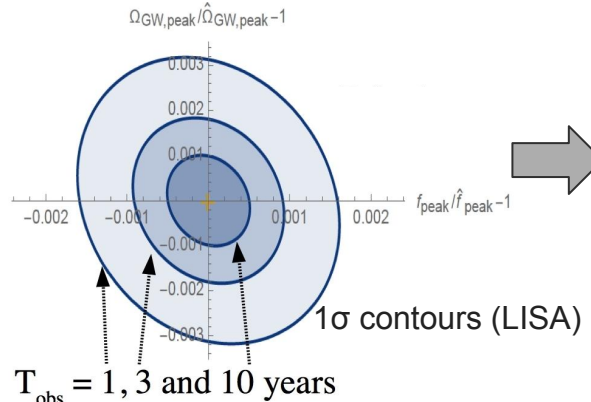
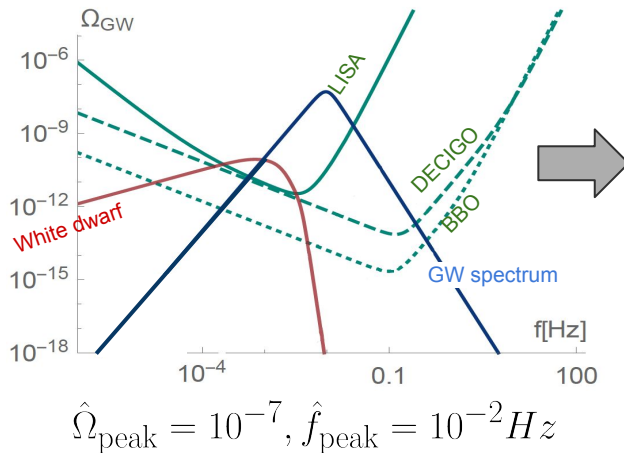
# Motivation

- ★ GW observations can be used to explore the NP effects for the first-order phase transition.

We can quantitatively discuss the expected uncertainties in the GW observations for NP effects by the Fisher matrix analysis.

[K. Hashino, R. Jinno, M. Kakizaki, S. Kanemura, T. Takahashi and M. Takimoto, PRD 99 (2019) no.7, 075011 ]

(The Fisher matrix corresponds to the inverse of the covariance matrix.)



$\hat{\Omega}_{\text{peak}} = 10^{-7} \pm 3 \times 10^{-10}$ ,  
 $\hat{f}_{\text{peak}} = 10^{-2} \pm 1.5 \times 10^{-5} \text{ Hz}$

LISA (1 year)

LISA, White dwarf : [A. Klein et al., Phys. Rev. D93 no. 2, (2016) 024003],

DECIGO, BBO : [K. Yagi and N. Seto, Phys. Rev. D83 (2011) 044011]

How precisely can we measure the SMEFT operator effect by GW observation?

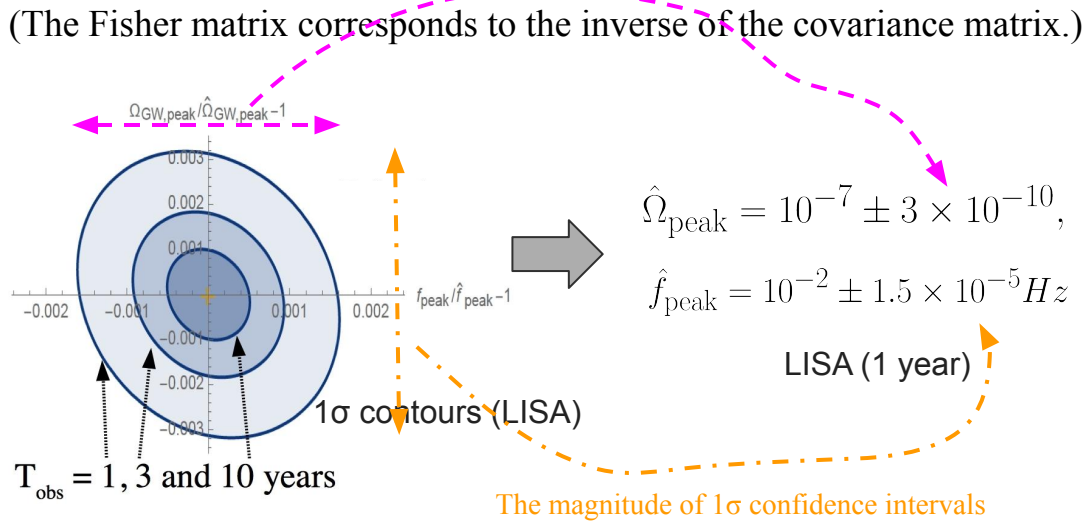
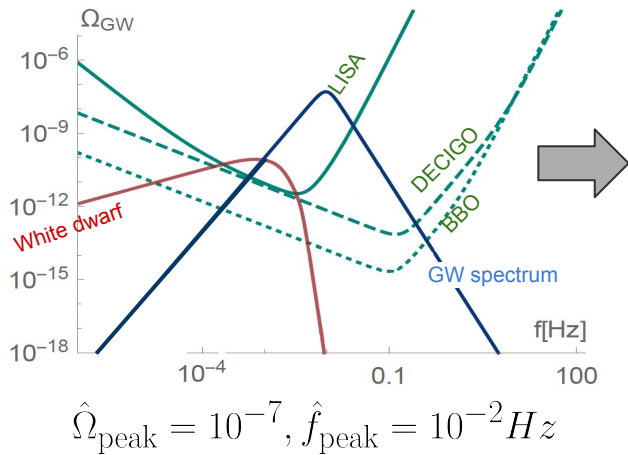
# Motivation

- ★ GW observations can be used to explore the NP effects for the first-order phase transition.

We can quantitatively discuss the expected uncertainties in the GW observations for NP effects by the Fisher matrix analysis.

[K. Hashino, R. Jinno, M. Kakizaki, S. Kanemura, T. Takahashi and M. Takimoto, PRD 99 (2019) no.7, 075011 ]

(The Fisher matrix corresponds to the inverse of the covariance matrix.)



LISA, White dwarf : [A. Klein et al., Phys. Rev. D93 no. 2, (2016) 024003],

DECIGO, BBO : [K. Yagi and N. Seto, Phys. Rev. D83 (2011) 044011]

How precisely can we measure the SMEFT operator effect by GW observation?

# SMEFT

$$\sqrt{2}H^T = (0, \varphi)$$

## ★ The Lagrangian of the SMEFT [B. Grzadkowski, M. Iskrzynski, M. Misiak, and J. Rosiek, JHEP 10 (2010) 085]

$$\mathcal{L}_{\text{SMEFT}} = \mathcal{L}_{\text{SM}} + \sum_i C_i \mathcal{O}_i$$

In this time, we consider the SMEFT operators involving Higgs and top-quarks.

Large Yukawa coupling compared to others

$$\left. \begin{aligned} (\mathcal{O}_{Hq}^{(1)})_{ij} &= (H^\dagger i \overleftrightarrow{D}_\mu H)(\bar{q}_i \gamma^\mu q_j), \\ (\mathcal{O}_{Hq}^{(3)})_{ij} &= (H^\dagger i \overleftrightarrow{D}_\mu^I H)(\bar{q}_i \tau^I \gamma^\mu q_j), \\ (\mathcal{O}_{Hu})_{ij} &= (H^\dagger i \overleftrightarrow{D}_\mu H)(\bar{u}_i \gamma^\mu u_j), \\ \mathcal{O}_H &= (H^\dagger H)^3, \\ \mathcal{O}_{H\square} &= (H^\dagger H)\square(H^\dagger H), \\ \mathcal{O}_{HD} &= (H^\dagger D^\mu H)^*(H^\dagger D_\mu H), \\ (\mathcal{O}_{uH})_{ij} &= (H^\dagger H)(\bar{q}_i u_j \tilde{H}), \end{aligned} \right\}$$

# SMEFT

$$\sqrt{2}H^T = (0, \varphi)$$

## ★ The Lagrangian of the SMEFT

[B. Grzadkowski, M. Iskrzynski, M. Misiak, and J. Rosiek, JHEP 10 (2010) 085]

$$\mathcal{L}_{\text{SMEFT}} = \mathcal{L}_{\text{SM}} + \sum_i C_i \mathcal{O}_i$$

In this time, we consider the SMEFT operators involving Higgs and top-quarks.

Large Yukawa coupling compared to others

$$\begin{aligned} (\mathcal{O}_{Hq}^{(1)})_{ij} &= (H^\dagger i \overleftrightarrow{D}_\mu H)(\bar{q}_i \gamma^\mu q_j), \\ (\mathcal{O}_{Hq}^{(3)})_{ij} &= (H^\dagger i \overleftrightarrow{D}_\mu^I H)(\bar{q}_i \tau^I \gamma^\mu q_j), \\ (\mathcal{O}_{Hu})_{ij} &= (H^\dagger i \overleftrightarrow{D}_\mu H)(\bar{u}_i \gamma^\mu u_j), \end{aligned}$$

The neutral Higgs field in the derivative  $\mathcal{O}_H = (H^\dagger H)$  of these operators cancels.

$$\begin{aligned} \mathcal{O}_{H\square} &= (H^\dagger H)\square(H^\dagger H), \\ \mathcal{O}_{HD} &= (H^\dagger D^\mu H)^*(H^\dagger D_\mu H), \\ (\mathcal{O}_{uH})_{ij} &= (H^\dagger H)(\bar{q}_i u_j \tilde{H}), \end{aligned}$$

# SMEFT

$$\sqrt{2}H^T = (0, \varphi)$$

## ★ The Lagrangian of the SMEFT [B. Grzadkowski, M. Iskrzynski, M. Misiak, and J. Rosiek, JHEP 10 (2010) 085]

$$\mathcal{L}_{\text{SMEFT}} = \mathcal{L}_{\text{SM}} + \sum_i C_i \mathcal{O}_i$$

In this time, we consider the SMEFT operators involving Higgs and top-quarks.

$$\Delta \mathcal{L}_{\text{SMEFT}} = \frac{1}{8} C_H \varphi^6$$

It is a dominant effect on the Higgs potential.

[C. Grojean, G. Servant, and J. D. Wells, Phys. Rev. D 71 (2005) 036001, D. Bodeker, L. Fromme, S. J. Huber, and M. Seniuch, JHEP 02 (2005) 026 and so on.]

$$(\mathcal{O}_{Hq}^{(1)})_{ij} = (H^\dagger i \overleftrightarrow{D}_\mu H)(\bar{q}_i \gamma^\mu q_j),$$

$$(\mathcal{O}_{Hq}^{(3)})_{ij} = (H^\dagger i \overleftrightarrow{D}_\mu^I H)(\bar{q}_i \tau^I \gamma^\mu q_j),$$

$$(\mathcal{O}_{Hu})_{ij} = (H^\dagger i \overleftrightarrow{D}_\mu H)(\bar{u}_i \gamma^\mu u_j),$$

$$\boxed{\mathcal{O}_H = (H^\dagger H)^3},$$

$$\mathcal{O}_{H\square} = (H^\dagger H) \square (H^\dagger H),$$

$$\mathcal{O}_{HD} = (H^\dagger D^\mu H)^* (H^\dagger D_\mu H),$$

$$(\mathcal{O}_{uH})_{ij} = (H^\dagger H)(\bar{q}_i u_j \tilde{H}),$$

# SMEFT

$$\sqrt{2}H^T = (0, \varphi)$$

## ★ The Lagrangian of the SMEFT

[B. Grzadkowski, M. Iskrzynski, M. Misiak, and J. Rosiek, JHEP 10 (2010) 085]

$$\mathcal{L}_{\text{SMEFT}} = \mathcal{L}_{\text{SM}} + \sum_i C_i \mathcal{O}_i \quad \left. \begin{array}{l} (\mathcal{O}_{Hq}^{(1)})_{ij} = (H^\dagger i \overleftrightarrow{D}_\mu H)(\bar{q}_i \gamma^\mu q_j), \\ (\mathcal{O}_{Hq}^{(3)})_{ij} = (H^\dagger i \overleftrightarrow{D}_\mu^I H)(\bar{q}_i \tau^I \gamma^\mu q_j), \\ (\mathcal{O}_{Hu})_{ij} = (H^\dagger i \overleftrightarrow{D}_\mu H)(\bar{u}_i \gamma^\mu u_j), \\ \mathcal{O}_H = (H^\dagger H)^3, \\ \mathcal{O}_{H\square} = (H^\dagger H)\square(H^\dagger H), \\ \mathcal{O}_{HD} = (H^\dagger D^\mu H)^*(H^\dagger D_\mu H), \\ (\mathcal{O}_{uH})_{ij} = (H^\dagger H)(\bar{q}_i u_j \tilde{H}), \end{array} \right\}$$

In this time, we consider the SMEFT operators involving Higgs and top-quarks.

$$\Delta \mathcal{L}_{\text{SMEFT}} = \frac{1}{4} C_{HD} \varphi^2 (\partial_\mu \varphi)^2 - C_{H\square} \varphi^2 (\partial_\mu \varphi)^2$$

These effects contribute to the Higgs potential by the wave function renormalization.

# SMEFT

$$\sqrt{2}H^T = (0, \varphi)$$

## ★ The Lagrangian of the SMEFT

[B. Grzadkowski, M. Iskrzynski, M. Misiak, and J. Rosiek, JHEP 10 (2010) 085]

$$\mathcal{L}_{\text{SMEFT}} = \mathcal{L}_{\text{SM}} + \sum_i C_i \mathcal{O}_i \quad \left. \begin{array}{l} (\mathcal{O}_{Hq}^{(1)})_{ij} = (H^\dagger i \overleftrightarrow{D}_\mu H)(\bar{q}_i \gamma^\mu q_j), \\ (\mathcal{O}_{Hq}^{(3)})_{ij} = (H^\dagger i \overleftrightarrow{D}_\mu^I H)(\bar{q}_i \tau^I \gamma^\mu q_j), \\ (\mathcal{O}_{Hu})_{ij} = (H^\dagger i \overleftrightarrow{D}_\mu H)(\bar{u}_i \gamma^\mu u_j), \\ \mathcal{O}_H = (H^\dagger H)^3, \\ \mathcal{O}_{H\square} = (H^\dagger H)\square(H^\dagger H), \\ \mathcal{O}_{HD} = (H^\dagger D^\mu H)^*(H^\dagger D_\mu H), \\ (\mathcal{O}_{uH})_{ij} = (H^\dagger H)(\bar{q}_i u_j \tilde{H}), \end{array} \right\}$$

In this time, we consider the SMEFT operators involving Higgs and top-quarks.

$$\Delta \mathcal{L}_{\text{SMEFT}} = C_{uH} \cdot \frac{3}{32\pi^2} Y_t \left( 14 - 6 \ln \frac{m_t^2}{v^2} \right) \cdot \frac{1}{2} \varphi^2 (\partial_\mu \varphi)^2 - \Delta V_{c_{uH}}$$

It contributes to the Higgs potential by the top-quark one-loop effects.

$$\Delta V_{c_{uH}} = -C_{uH} \cdot \frac{3}{32\pi^2} Y_t^3 \varphi^6 \left( -1 + \ln \frac{Y_t^2 \varphi^2}{2v^2} \right)$$

# SMEFT

- ★ The Higgs potential up to the first order of the Wilson coefficients

$$V = \frac{1}{2}\mu^2\varphi^2 + \frac{1}{4} \left( \lambda - \frac{4}{3}c_{\text{kin}}^{(0)}\mu^2 \right) \varphi^4 - \frac{1}{4}c_{\text{kin}}^{(1)}\mu^2\varphi^5 + \frac{1}{6} \left( -\frac{3}{4}C_H - 2c_{\text{kin}}^{(0)}\lambda - \frac{6}{5}c_{\text{kin}}^{(2)}\mu^2 \right) \varphi^6 + \Delta V_{c_{uH}}$$

$$c_{\text{kin}}^{(0)} = \frac{1}{4}C_{HD} - C_{H\square} + \frac{1}{2}C_{uH} \cdot \frac{3}{32\pi^2}Y_t \left( 14 - 6 \ln \frac{m_t^2}{v^2} \right),$$

$$c_{\text{kin}}^{(1)} = \frac{1}{2}C_{uH} \cdot \frac{3}{32\pi^2}Y_t \left( -\frac{28}{v} \right),$$

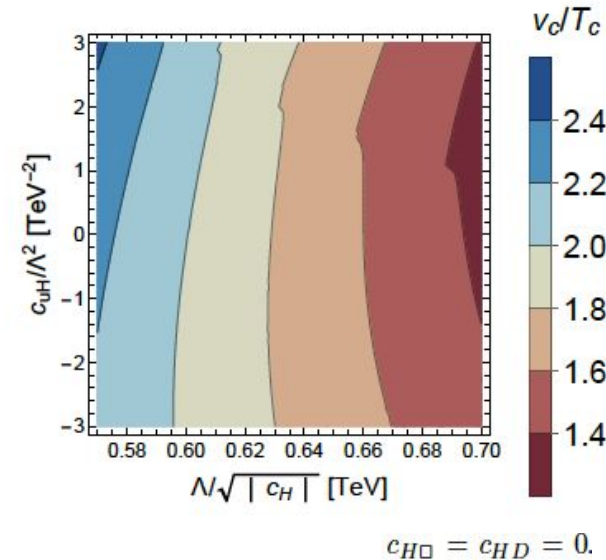
$$c_{\text{kin}}^{(2)} = \frac{1}{2}C_{uH} \cdot \frac{3}{32\pi^2}Y_t \left( \frac{8}{v^2} \right).$$

$$\Delta V_{c_{uH}} = -C_{uH} \cdot \frac{3}{32\pi^2}Y_t^3\varphi^6 \left( -1 + \ln \frac{Y_t^2\varphi^2}{2v^2} \right)$$

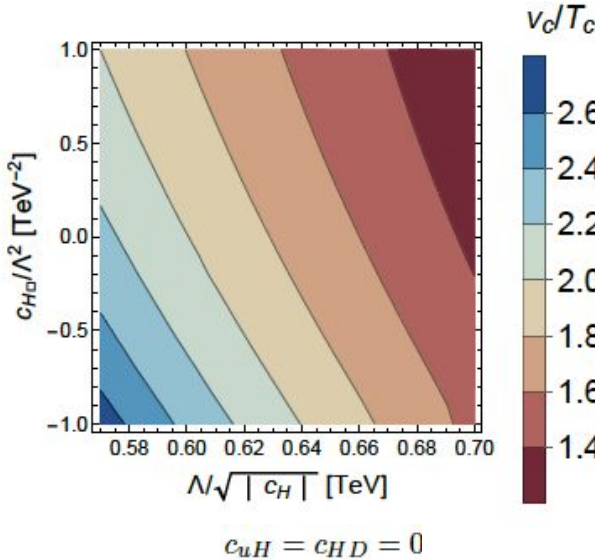
By using this potential, we can evaluate the first-order EWPT.

# First-order EWPT

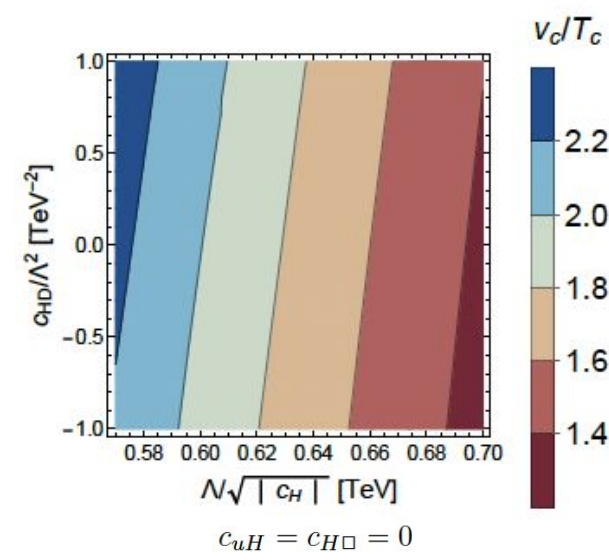
- ★ The results of  $v_c/T_c$  for normalized  $(C_H, C_{uH})$ ,  $(C_H, C_{H\square})$  and  $(C_H, C_{HD})$ .



$$c_{H\square} = c_{HD} = 0.$$



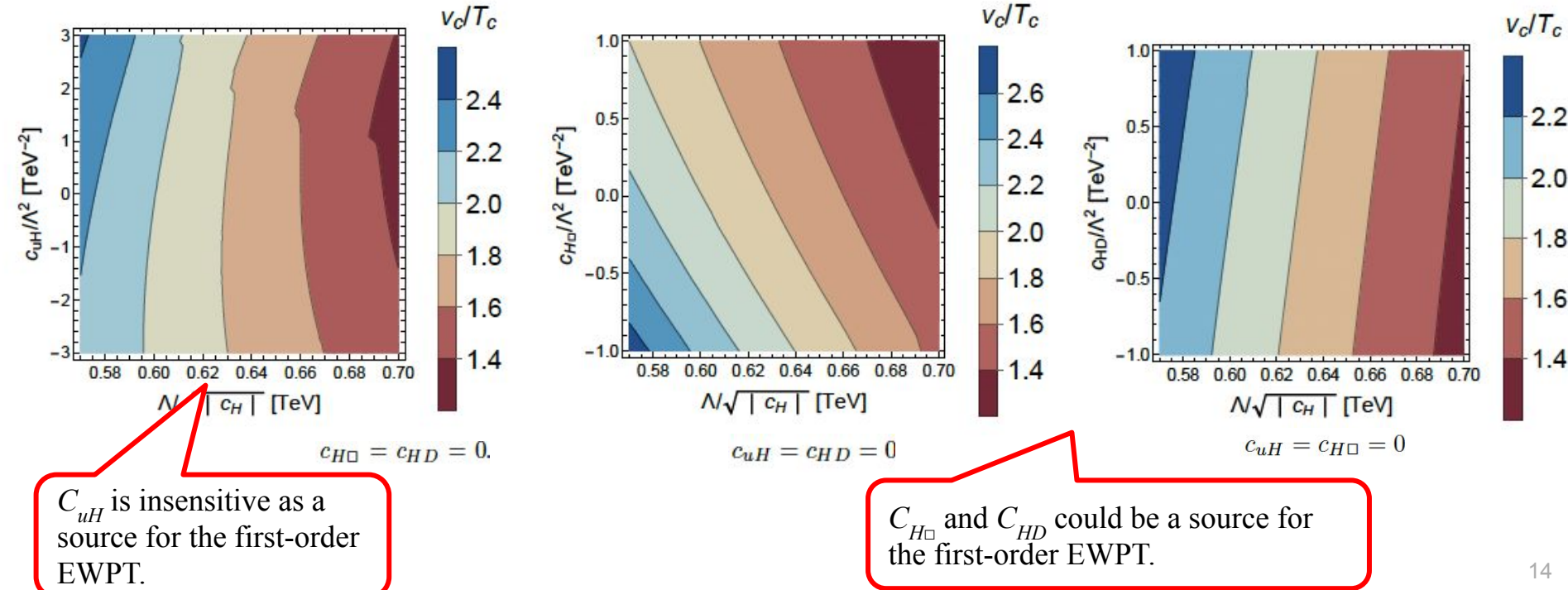
$$c_{uH} = c_{HD} = 0$$



$$c_{uH} = c_{H\square} = 0$$

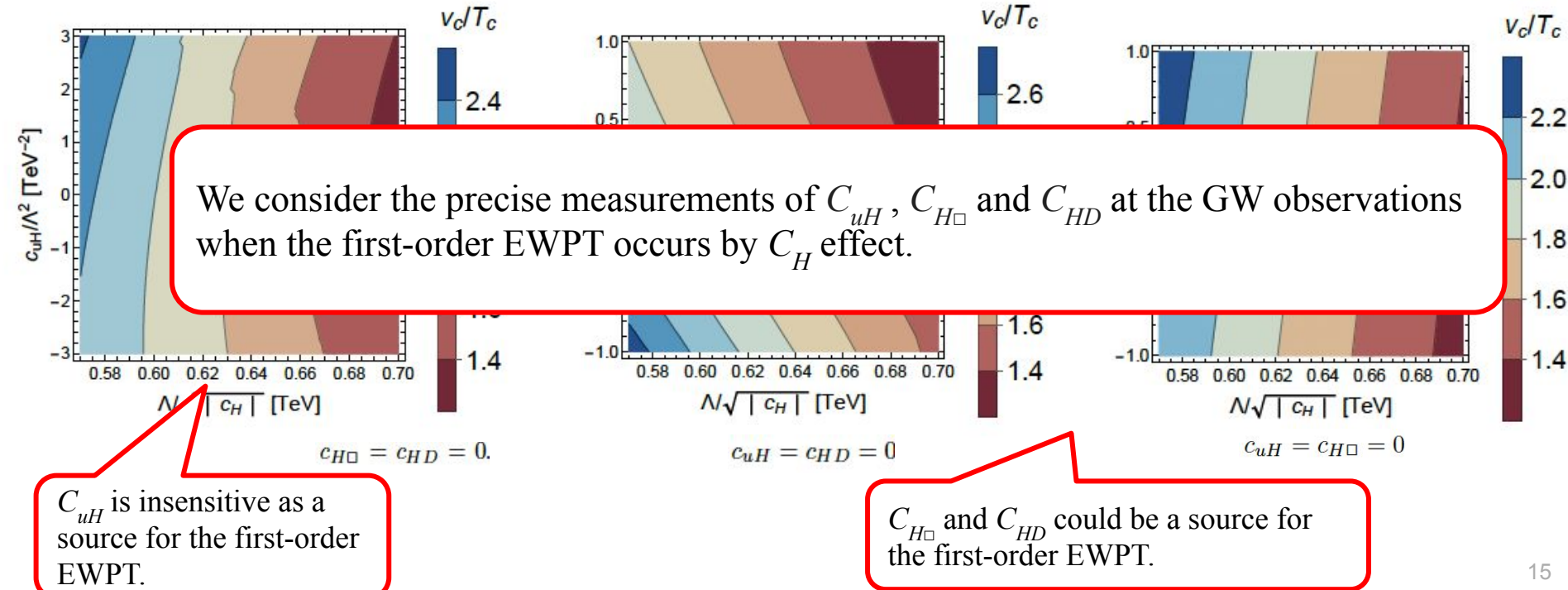
# First-order EWPT

- ★ The results of  $v_c/T_c$  for normalized  $(C_H, C_{uH})$ ,  $(C_H, C_{H\square})$  and  $(C_H, C_{HD})$ .



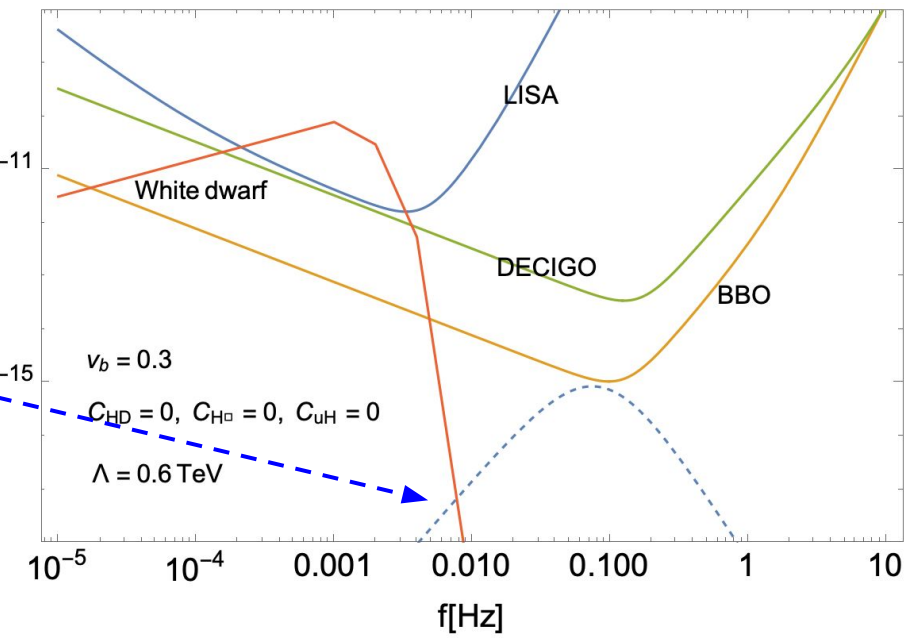
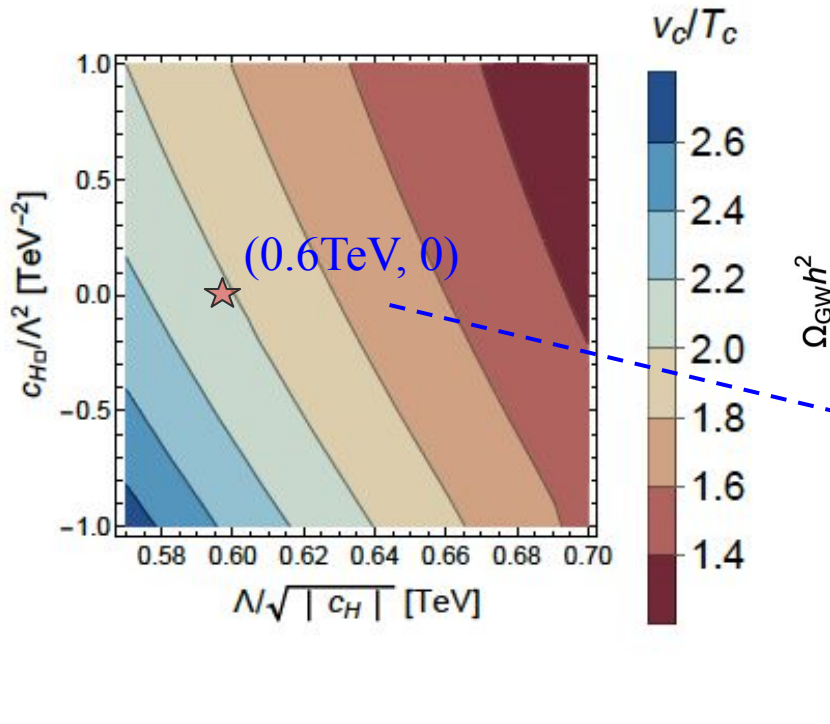
# First-order EWPT

- ★ The results of  $v_c/T_c$  for normalized  $(C_H, C_{uH})$ ,  $(C_H, C_{H\square})$  and  $(C_H, C_{HD})$ .



# First-order EWPT

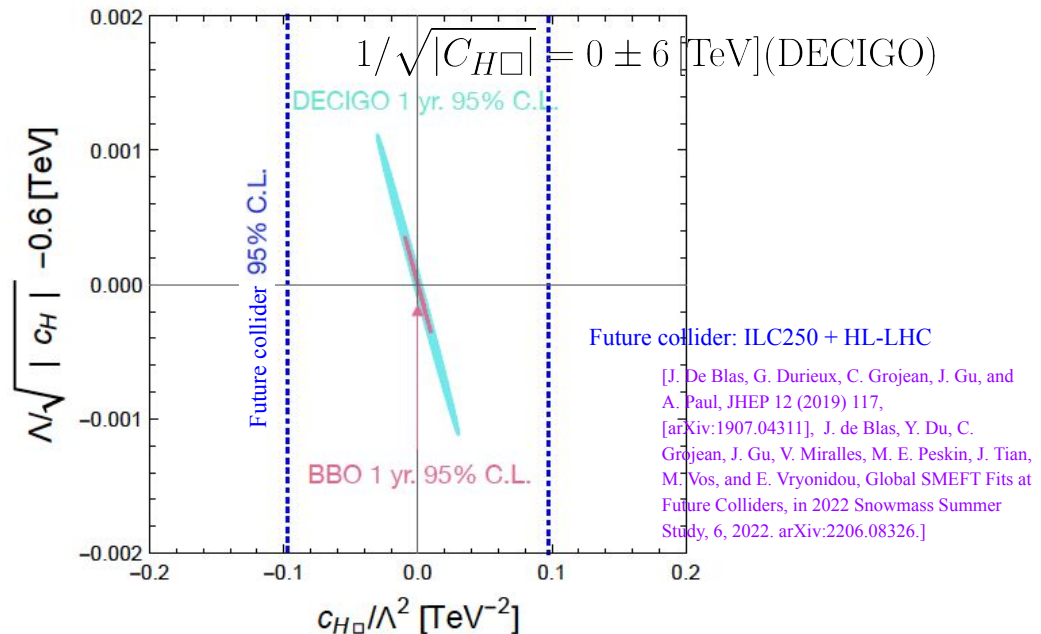
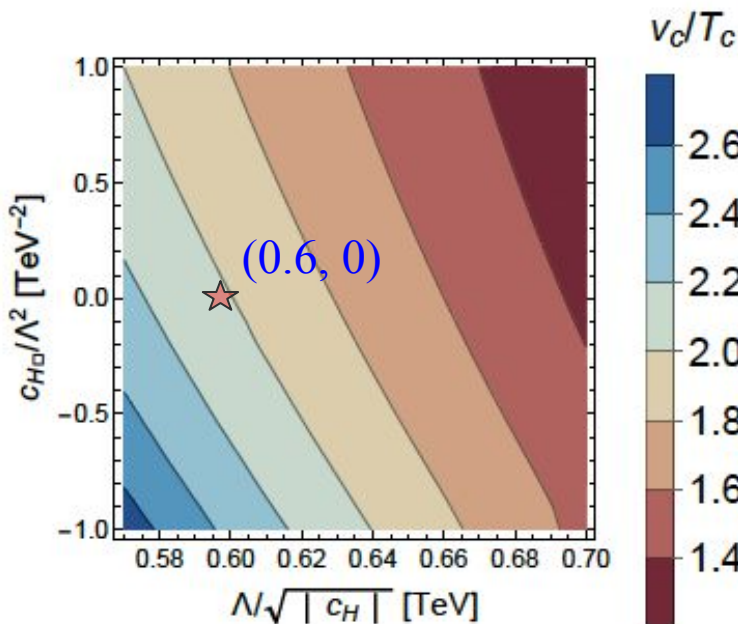
- ★ Example of the expected uncertainty for  $(C_H, C_{H\square})$  at the GW observation



$$C_H = 0.6 \text{ TeV}, C_{H\square} = 0$$

# First-order EWPT

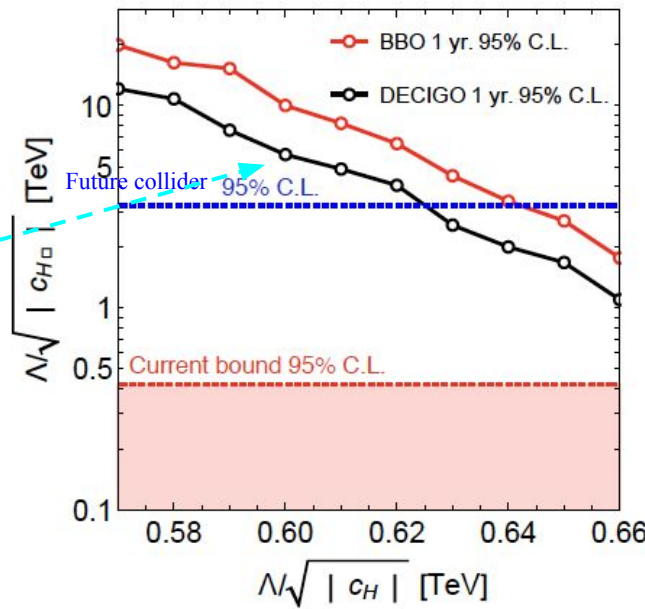
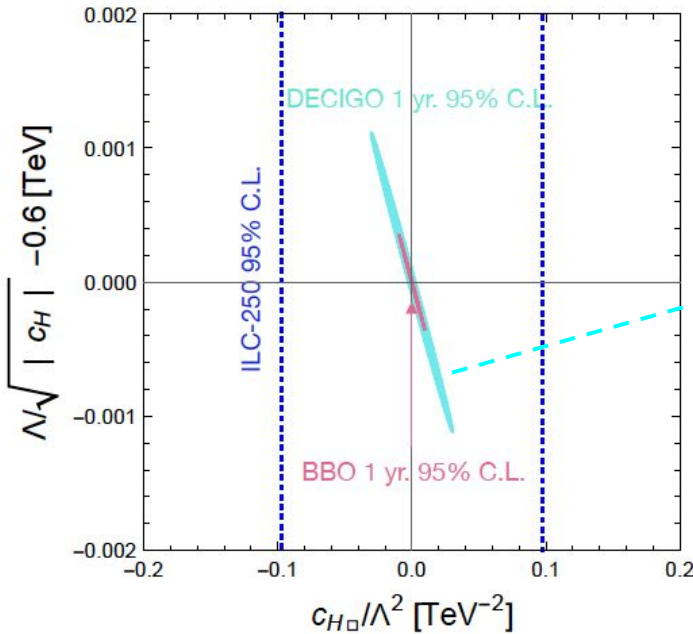
- ★ Example of the expected uncertainty for  $(C_H, C_{H\square})$  at the GW observation



95% C.L. confidence regions for DECIGO and BBO with 1-year statistics, assuming the central values of the benchmark point.

# First-order EWPT

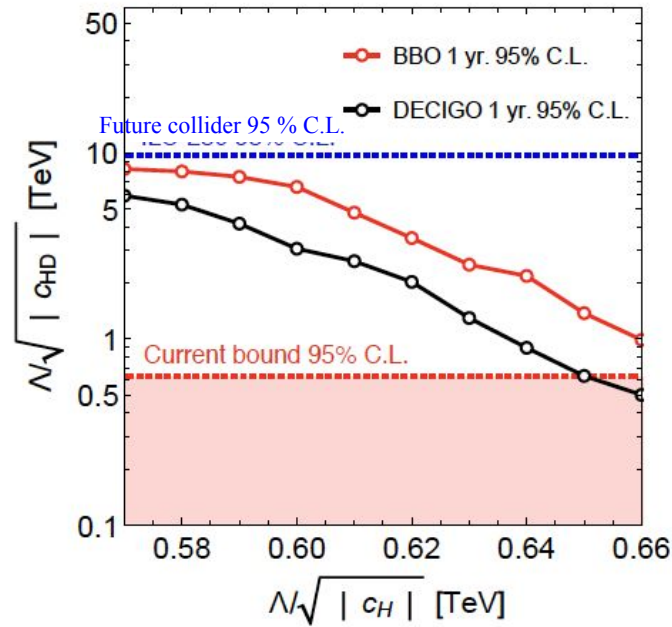
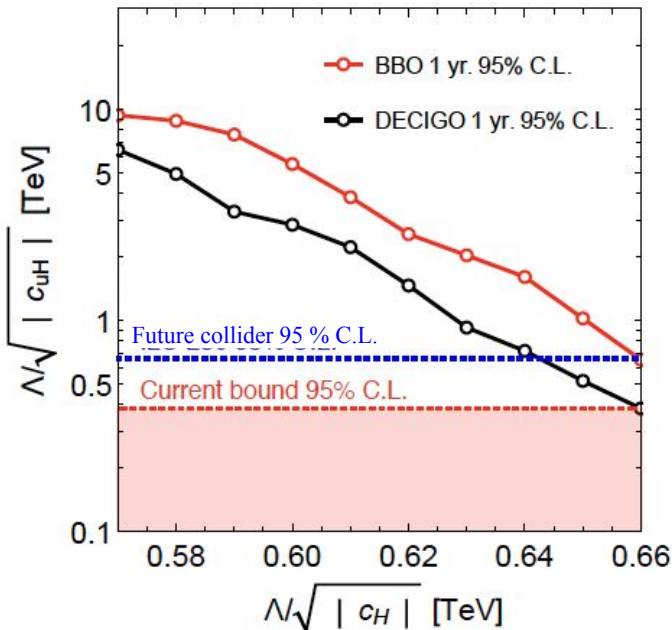
- ★ Example of the expected uncertainty for  $(C_H, C_{H\square})$  at the GW observation



The magnitude of 95% C.L. confidence intervals of vertical axis ( $C_{H\square}$ ).

# First-order EWPT

- ★ Expected uncertainties for other effects at the GW observation



DECIGO and the BBO experiments can be sensitive to the SMEFT effects, such as  $C_{uH}$  and  $C_{H\Box}$ , once the SFO-EWPT arises.

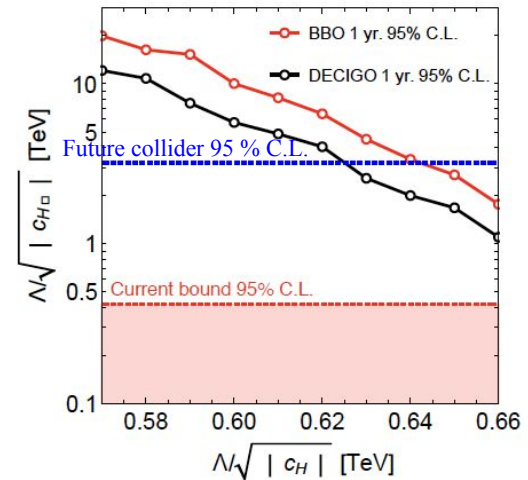
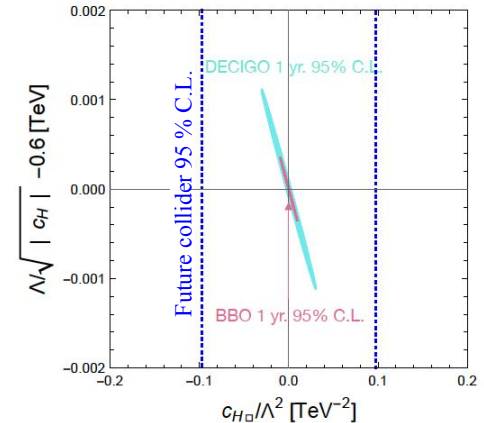
# Summary

- ★ New physics effects are required to realize the strongly first-order EWPT.
- ★ In this time, we consider the SMEFT and discuss the dimension-six operator effects on the spectrum of GWs.

$$\mathcal{O}_H, \mathcal{O}_{H\square}, \mathcal{O}_{HD}, \mathcal{O}_{uH},$$

- ★ DECIGO and the BBO experiments can be sensitive to the SMEFT effects, once the SFO-EWPT arises.

In particular, its sensitivities to the operators  $\mathcal{O}_{uH}$  and  $\mathcal{O}_{u\square}$  are potentially higher than future collider experiments.



# Backup

# Fisher matrix analysis

## ❖ Likelihood function

$$\delta\chi^2(\{p\}, \{\hat{p}\}) := 2T_{\text{obs}} \sum_{(I,I')} \int_0^\infty df \frac{\Gamma_{II'}^2(f) [S_h(f, \{p\}) - S_h(f, \{\hat{p}\})]^2}{\sigma_{II'}^2(f)}. \quad S_h(f) = \frac{3H_0^2}{2\pi^2} \frac{1}{f^3} \Omega_{\text{GW}}(f)$$

Noise for detection of GW:  $\sigma_{II'}^2(f) = [S_I(f) + \Gamma_{II}(f)S_h(f, \{\hat{p}\})] [S_{I'}(f) + \Gamma_{II'}(f)S_h(f, \{\hat{p}\})] + \Gamma_{II'}^2(f)S_h^2(f, \{\hat{p}\})$

$S_h(f, \{p\})$ : GW spectrum for parameter set  $\{p\}$ ,

$\Gamma_{II'}$  is the overlap reduction function.

$S_{\text{eff}}$ : Effective sensitivity of interferometers,

$\{\hat{p}\}$ : Fiducial parameter set,  $T_{\text{obs}}$ : Observation period

Taylor expansion

$$\delta\chi^2(\{p\}, \{\hat{p}\}) \simeq \mathcal{F}_{ab}(p_a - \hat{p}_a)(p_b - \hat{p}_b) \quad \mathcal{F}_{ab} = 2T_{\text{obs}} \sum_{(I,I')} \int_0^\infty df \frac{\Gamma_{II'}^2(f) \partial_{p_a} S_h(f, \{\hat{p}\}) \partial_{p_b} S_h(f, \{\hat{p}\})}{\sigma_{II'}^2(f)}$$

$$S_{\text{eff}}(f) = \left[ \sum_{(I,I')} \frac{\Gamma_{II'}^2(f)}{\sigma_{II'}^{(\text{null})2}(f)} \right]^{-1/2}$$

[N. Seto, Phys. Rev. D 73, 063001 (2006)]

[E. Thrane and J. D. Romano, Phys. Rev. D 88, no. 12, 124032 (2013)]

# Fisher matrix analysis

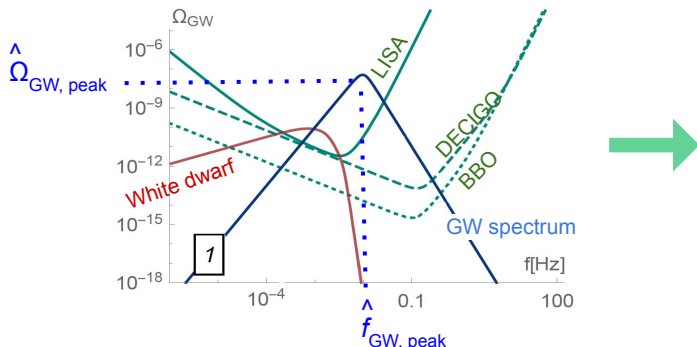
## ❖ Likelihood function

$$\delta\chi^2(\{p\}, \{\hat{p}\}) = 2T_{\text{obs}} \int_0^\infty df \frac{[S_h(f, \{p\}) - S_h(f, \{\hat{p}\})]^2}{[S_{\text{eff}}(f) + S_h(f, \{\hat{p}\})]^2}$$

Taylor expansion →  $\delta\chi^2(\{p\}, \{\hat{p}\}) \simeq \mathcal{F}_{ab}(p_a - \hat{p}_a)(p_b - \hat{p}_b)$

$$\mathcal{F}_{ab} = 2T_{\text{obs}} \int_0^\infty df \frac{\partial_{p_a} S_h(f, \{\hat{p}\}) \partial_{p_b} S_h(f, \{\hat{p}\})}{[S_{\text{eff}}(f) + S_h(f, \{\hat{p}\})]^2}$$

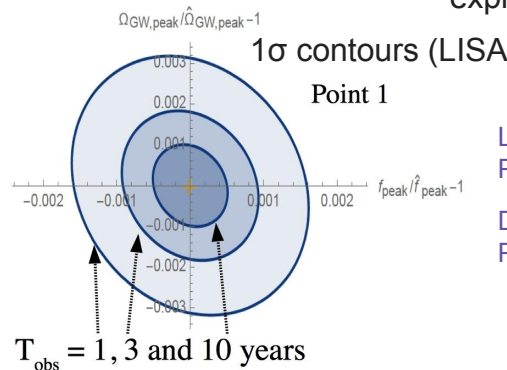
## ❖ Sample point



$S_h(f, \{p\})$  : GW spectrum for parameter set  $\{p\}$ ,  
 $S_{\text{eff}}$  : Effective sensitivity of interferometers,  
 $\{\hat{p}\}$  : Fiducial parameter set,  $T_{\text{obs}}$  : Observation period

The inverse matrix of  $\mathcal{F}_{ab}$  is the covariance matrix.

(We assume that we can apply the expression to one detector (LISA).)



LISA, White dwarf : [A. Klein et al., Phys. Rev. D93 no. 2, (2016) 024003]

DECIGO, BBO : [K. Yagi and N. Seto, Phys. Rev. D83 (2011) 044011]

❖ The expected constraints on the GW spectrum propagate to the parameters in the model.

# Fisher matrix analysis

## ❖ Effective sensitivity

- LISA

$$S_{\text{eff}}(f) = \frac{20}{3} \frac{4S_{\text{acc}}(f) + S_{\text{sn}}(f) + S_{\text{omn}}(f)}{L^2} \left[ 1 + \left( \frac{f}{0.41c/2L} \right)^2 \right],$$

with  $L = 5 \times 10^9$  m and

$$S_{\text{acc}}(f) = 9 \times 10^{-30} \frac{1}{(2\pi f/1\text{Hz})^4} \left( 1 + \frac{10^{-4}}{f/1\text{Hz}} \right) \text{ m}^2\text{Hz}^{-1},$$

$$S_{\text{sn}}(f) = 2.96 \times 10^{-23} \text{ m}^2\text{Hz}^{-1},$$

$$S_{\text{omn}}(f) = 2.65 \times 10^{-23} \text{ m}^2\text{Hz}^{-1}.$$

[A. Klein et al., Phys. Rev. D93 no. 2, (2016) 024003]

- DECIGO

$$S_{\text{eff}}(f) = \left[ 7.05 \times 10^{-48} [1 + (f/f_p)^2] + 4.8 \times 10^{-51} \frac{(f/1\text{Hz})^{-4}}{1 + (f/f_p)^2} + 5.33 \times 10^{-52} (f/1\text{Hz})^{-4} \right] \text{ Hz}^{-1},$$

with  $f_p = 7.36$  Hz.

- BBO

$$S_{\text{eff}}(f) = [2.00 \times 10^{-49} (f/1\text{Hz})^2 + 4.58 \times 10^{-49} + 1.26 \times 10^{-52} (f/1\text{Hz})^{-4}] \text{ Hz}^{-1}.$$

[K. Yagi and N. Seto, Phys. Rev. D83 (2011) 044011]

# Fisher matrix analysis

- ❖ Noise for the white dwarf [A. Klein et al., Phys. Rev. D93 no. 2, (2016) 024003]

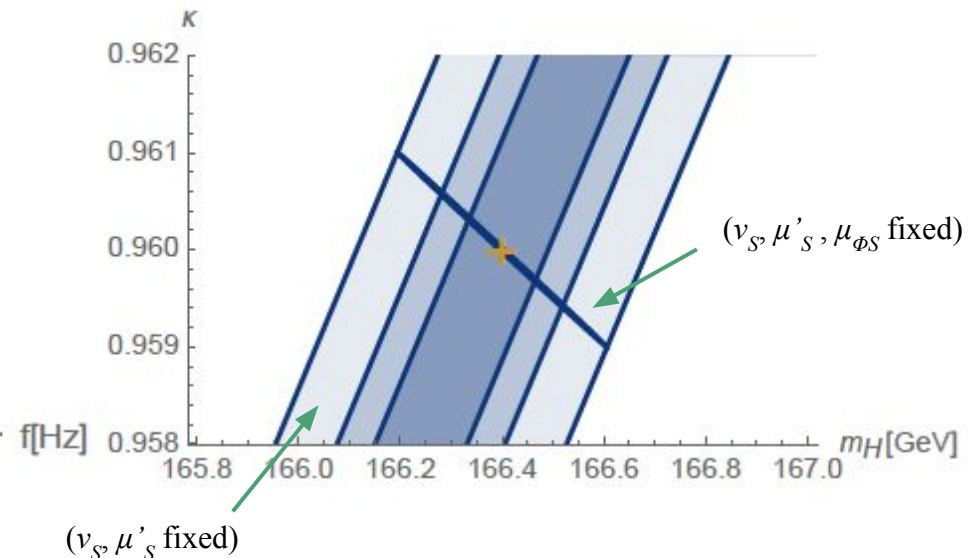
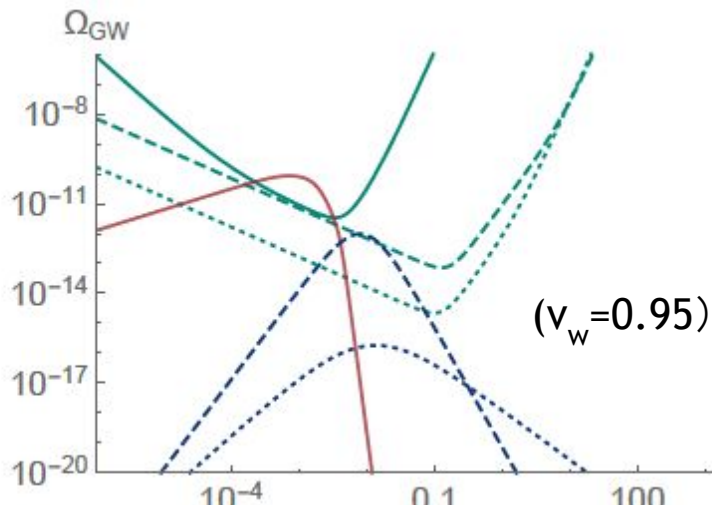
$$S'_{\text{WD}}(f) = \begin{cases} (20/3)(f/1 \text{ Hz})^{-2.3} \times 10^{-44.62} \text{ Hz}^{-1} & \equiv S_{\text{WD}}^{(1)}(f) \quad (10^{-5} \text{ Hz} < f < 10^{-3} \text{ Hz}), \\ (20/3)(f/1 \text{ Hz})^{-4.4} \times 10^{-50.92} \text{ Hz}^{-1} & \equiv S_{\text{WD}}^{(2)}(f) \quad (10^{-3} \text{ Hz} < f < 10^{-2.7} \text{ Hz}), \\ (20/3)(f/1 \text{ Hz})^{-8.8} \times 10^{-62.8} \text{ Hz}^{-1} & \equiv S_{\text{WD}}^{(3)}(f) \quad (10^{-2.7} \text{ Hz} < f < 10^{-2.4} \text{ Hz}), \\ (20/3)(f/1 \text{ Hz})^{-20.0} \times 10^{-89.68} \text{ Hz}^{-1} & \equiv S_{\text{WD}}^{(4)}(f) \quad (10^{-2.4} \text{ Hz} < f < 10^{-2} \text{ Hz}). \end{cases}$$

$$S_{\text{WD}}(f) = \frac{1}{1/S_{\text{WD}}^{(1)}(f) + 1/S_{\text{WD}}^{(2)}(f) + 1/S_{\text{WD}}^{(3)}(f) + 1/S_{\text{WD}}^{(4)}(f)}$$

$$S_{\text{WD}} \simeq \max(S_{\text{WD}}^{(1)}, S_{\text{WD}}^{(2)}, S_{\text{WD}}^{(3)}, S_{\text{WD}}^{(4)})$$

# Fisher matrix analysis

- ❖ The expected uncertainties for LISA at Fiducial point ( $m_H$ ,  $\kappa$ ) = (166.4 GeV, 0.96) (Blue ellipses and bands)



# Fisher matrix analysis

- ❖ Noise for binary neutron stars and binary black holes (Stochastic GW)

[Virgo, LIGO Scientific Collaboration, B. P. Abbott et al., arXiv:1710.05837 [gr-qc]]

$$S_{\text{NSBH}}(f) = \frac{3H_0^2}{2\pi^2} \frac{1}{f^3} \times 1.8 \times 10^{-8} \left( \frac{f}{25 \text{ Hz}} \right)^{\frac{2}{3}} \quad 10 \text{ Hz} < f < 10^3 \text{ Hz}$$

→ This noise does not affect our analysis, because frequency of the noise is small.

(We tried to extrapolate the noise to 1 Hz, but our result doesn't change.)

# $\varphi$ part of the Lagrangian

$$\mathcal{L}_\varphi = c_{\text{kin}} \varphi^2 (\partial_\mu \varphi)^2 + \frac{1}{8} C_H \varphi^6 - \Delta V_{c_{uH}},$$



$$\varphi \rightarrow \varphi - \frac{1}{3} c_{\text{kin}}^{(0)} \cdot \varphi^3 - \frac{1}{4} c_{\text{kin}}^{(1)} \cdot \varphi^4 - \frac{1}{5} c_{\text{kin}}^{(2)} \cdot \varphi^5 + \mathcal{O}(c_{\text{kin}}^2),$$

$$c_{\text{kin}} = c_{\text{kin}}^{(0)} + c_{\text{kin}}^{(1)} \cdot \varphi + c_{\text{kin}}^{(2)} \cdot \varphi^2,$$

$$c_{\text{kin}}^{(0)} = \frac{1}{4} C_{HD} - C_{H\square} + \frac{1}{2} C_{uH} \cdot \frac{3}{32\pi^2} Y_t \left( 14 - 6 \ln \frac{m_t^2}{v^2} \right),$$

$$c_{\text{kin}}^{(1)} = \frac{1}{2} C_{uH} \cdot \frac{3}{32\pi^2} Y_t \left( -\frac{28}{v} \right),$$

$$c_{\text{kin}}^{(2)} = \frac{1}{2} C_{uH} \cdot \frac{3}{32\pi^2} Y_t \left( \frac{8}{v^2} \right).$$

$$\mathcal{L}_\varphi = \frac{1}{2} (\partial_\mu \varphi)^2 - V,$$

$$V = \frac{1}{2} \mu^2 \varphi^2 + \frac{1}{4} \left( \lambda - \frac{4}{3} c_{\text{kin}}^{(0)} \mu^2 \right) \varphi^4 - \frac{1}{4} c_{\text{kin}}^{(1)} \mu^2 \varphi^5 + \frac{1}{6} \left( -\frac{3}{4} C_H - 2 c_{\text{kin}}^{(0)} \lambda - \frac{6}{5} c_{\text{kin}}^{(2)} \mu^2 \right) \varphi^6 + \Delta V_{c_{uH}}$$

# First-order EWPT

$$V_{\text{eff}}(\varphi, 0) = \frac{1}{2}a_2\varphi^2 + \frac{1}{4}a_4\varphi^4 + \frac{1}{5}a_5\varphi^5 + \frac{1}{6}a_6\varphi^6$$

where

$$\begin{aligned} a_2 &= \mu^2, \quad a_4 = \lambda - \frac{4}{3}c_{\text{kin}}^{(0)}\mu^2, \quad a_5 = -\frac{5}{4}c_{\text{kin}}^{(1)}\mu^2, \\ a_6 &= -\frac{3}{4}C_H - 2c_{\text{kin}}^{(0)}\lambda - \frac{6}{5}c_{\text{kin}}^{(2)}\mu^2 - \frac{9}{16\pi^2}C_{uH}Y_t^3 \left( -1 + \ln \frac{Y_t^2\varphi^2}{2v^2} \right) \end{aligned}$$

$$\partial_\varphi V_{\text{eff}}(\varphi, 0)|_{\varphi=v} = a_2v + a_4v^3 + a_5v^4 + a_6v^5 = 0,$$

$$\partial_\varphi^2 V_{\text{eff}}(\varphi, 0)|_{\varphi=v} = a_2 + 3a_4v^2 + 4a_5v^3 + 5a_6v^4 = m_h^2.$$

→  $V_{\text{eff}}(\varphi, 0) = -\frac{1}{4}(m_h^2 - a_5v^3 - 2a_6v^4)\varphi^2 + \frac{1}{4}\left(\frac{m_h^2}{2v^2} - \frac{3}{2}a_5v - 2a_6v^2\right)\varphi^4 + \frac{1}{5}a_5\varphi^5 + \frac{1}{6}a_6\varphi^6$

$\downarrow$

$\frac{a_5}{2v} + a_6 \sim \frac{m_h^2}{2v^4} \simeq (685 \text{ GeV})^{-2}$

# First-order EWPT

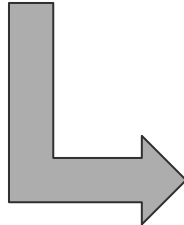
- ★ Potential with finite temperature effects.

$$c_{\text{kin}}^{(0)} = \frac{1}{4} C_{HD} - C_{H\square} + \frac{1}{2} C_{uH} \cdot \frac{3}{32\pi^2} Y_t \left( 14 - 6 \ln \frac{m_t^2}{v^2} \right),$$

$$c_{\text{kin}}^{(1)} = \frac{1}{2} C_{uH} \cdot \frac{3}{32\pi^2} Y_t \left( -\frac{28}{v} \right),$$

$$c_{\text{kin}}^{(2)} = \frac{1}{2} C_{uH} \cdot \frac{3}{32\pi^2} Y_t \left( \frac{8}{v^2} \right).$$

$$V_{\text{eff}}(\varphi, T) \sim \frac{1}{2} A_2 \varphi^2 - \frac{1}{2\sqrt{2}} E T \varphi^3 + \frac{1}{4} A_4 \varphi^4, \quad A_4 \equiv a_4 + 4a_5 \varphi/5 + 2a_6 \varphi^2/3$$



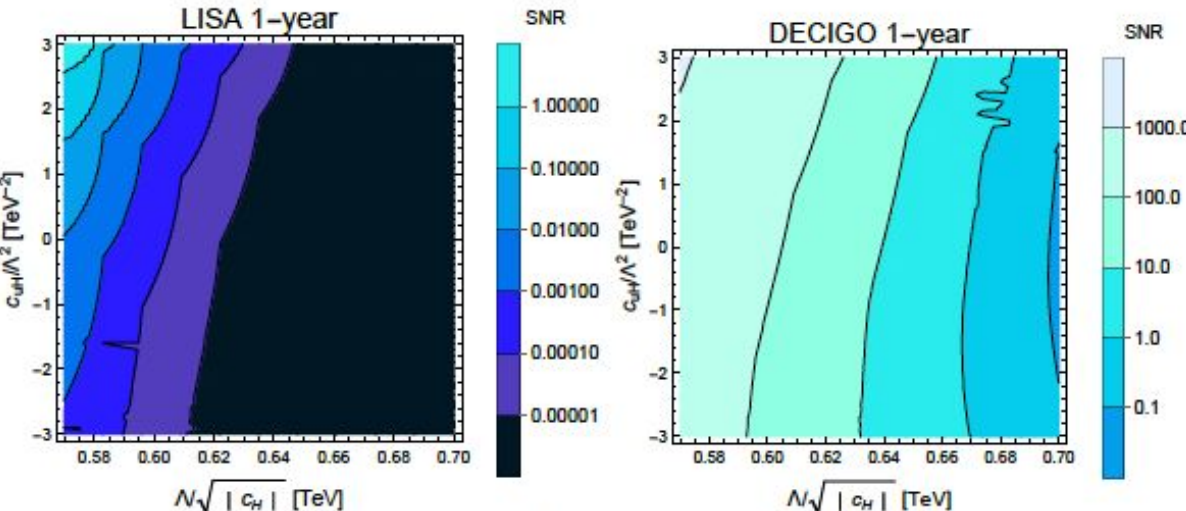
$$\frac{v_c}{T_c} = \frac{E}{\sqrt{2} A_4} \sim \frac{E}{\sqrt{2} \left( m_h^2 / (2v^2) - 3a_5 v/2 - 2a_6 v^2 \right)}$$

where

$$a_2 = \mu^2, \quad a_4 = \lambda - \frac{4}{3} c_{\text{kin}}^{(0)} \mu^2, \quad a_5 = -\frac{5}{4} c_{\text{kin}}^{(1)} \mu^2,$$

$$a_6 = -\frac{3}{4} C_H - 2c_{\text{kin}}^{(0)} \lambda - \frac{6}{5} c_{\text{kin}}^{(2)} \mu^2 - \frac{9}{16\pi^2} C_{uH} Y_t^3 \left( -1 + \ln \frac{Y_t^2 \varphi^2}{2v^2} \right)$$

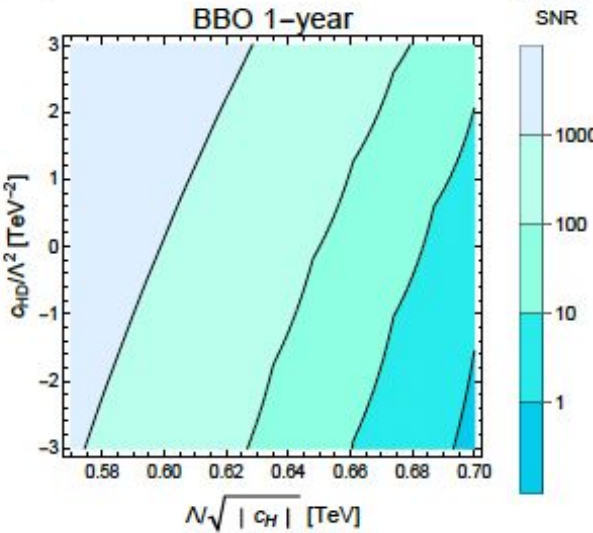
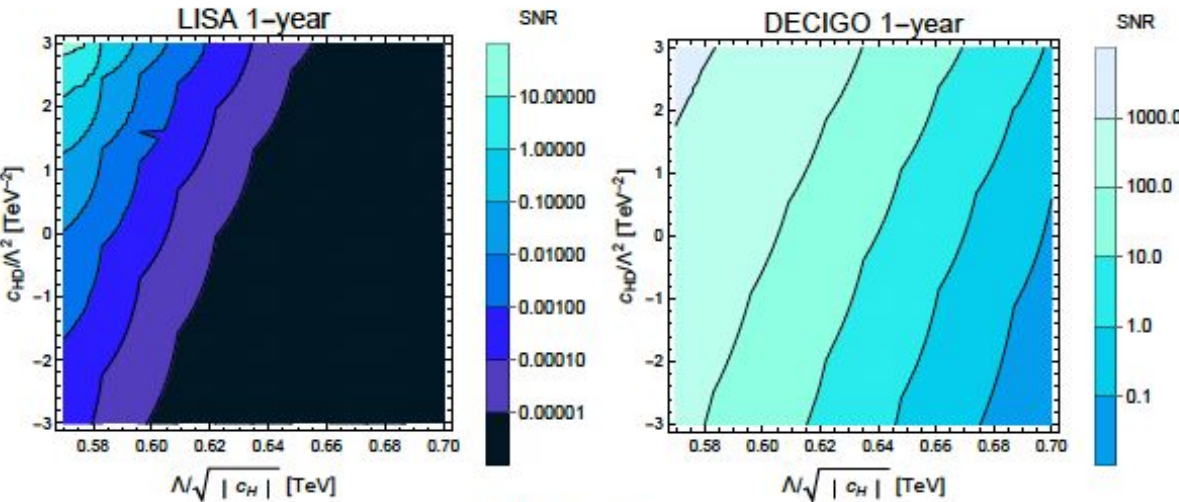
- ★ SNR results with respect to CH and CuH



$$\text{SNR} = \sqrt{\delta \times T_{\text{obs}} \int_0^{\infty} df \left[ \frac{\Omega_{\text{GW}}(f)}{\Omega_{\text{sen}}(f)} \right]^2}$$

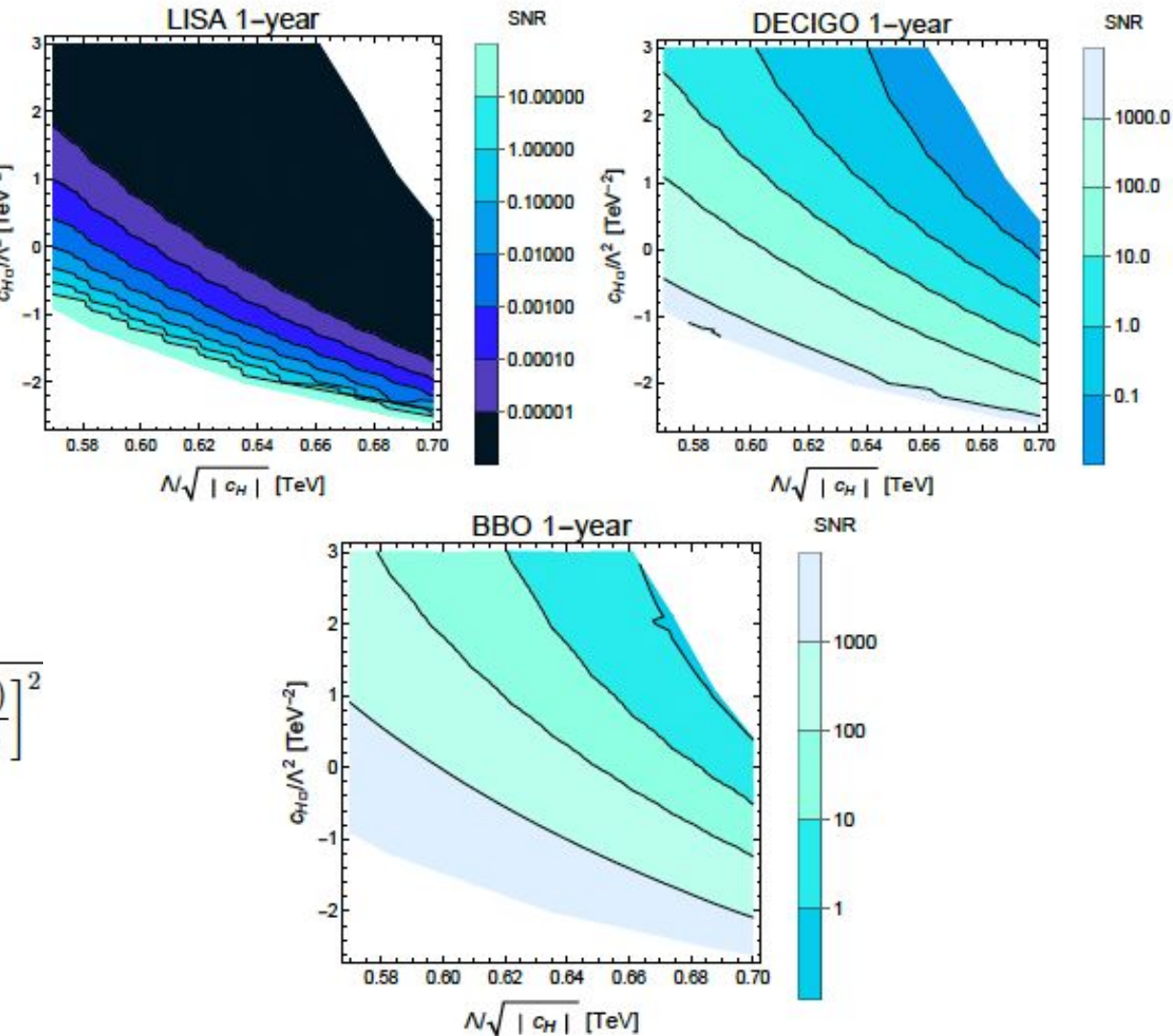
- ★ SNR results with respect to CH and CHD

$$\text{SNR} = \sqrt{\delta \times T_{\text{obs}} \int_0^{\infty} df \left[ \frac{\Omega_{\text{GW}}(f)}{\Omega_{\text{sen}}(f)} \right]^2}$$



- ★ SNR results with respect to CH and  $\text{CH}\square$

$$\text{SNR} = \sqrt{\delta \times T_{\text{obs}} \int_0^{\infty} df \left[ \frac{\Omega_{\text{GW}}(f)}{\Omega_{\text{sen}}(f)} \right]^2}$$



$$\begin{aligned}
\partial V_{\text{eff}}(v_{\text{SM}})/\partial \varphi &= \lim_{\Delta \rightarrow 0} \frac{V_{\text{eff}}(v_{\text{SM}} + \Delta) - V_{\text{eff}}(v_{\text{SM}})}{\Delta} \\
&= \lim_{\Delta \rightarrow 0} \frac{V_{\text{eff}}(v_{\text{SMEFT}} - \delta v + \Delta) - V_{\text{eff}}(v_{\text{SMEFT}} - \delta v)}{\Delta} \\
&= 0
\end{aligned}$$

$$\begin{aligned}
V_{\text{eff}}(v_{\text{SMEFT}} - \delta v + \Delta) &= V_{\text{eff}}(v_{\text{SMEFT}}) + \frac{\partial V_{\text{eff}}(v_{\text{SMEFT}})}{\partial \varphi} \cdot (-\delta v + \Delta) + \mathcal{O}((-\delta v + \Delta)^2) \\
&= V_{\text{eff}}(v_{\text{SMEFT}}) + \mathcal{O}((-\delta v + \Delta)^2)
\end{aligned}$$

$$\begin{aligned}
V_{\text{eff}}(v_{\text{SMEFT}} - \delta v) &= V_{\text{eff}}(v_{\text{SMEFT}}) + \frac{\partial V_{\text{eff}}(v_{\text{SMEFT}})}{\partial \varphi} \cdot (-\delta v) + \mathcal{O}((-\delta v)^2) \\
&= V_{\text{eff}}(v_{\text{SMEFT}}) + \mathcal{O}((-\delta v)^2)
\end{aligned}$$

# GW from first-order phase transition

- ★ The bubble dynamics is determined by the following parameters:

$$T_t, \alpha, \beta/H, v_b$$

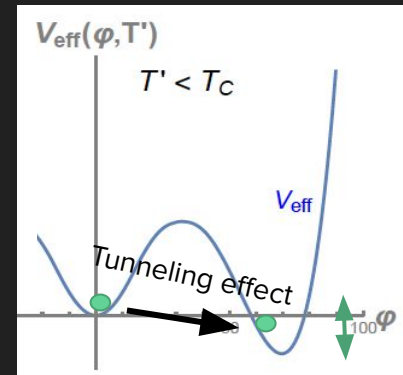
**The GW spectrum from first-order EWPT can be featured by these parameters.**

- (1)  $T_t$ : Transition temperature (The temperature of the Universe just after the phase transition.)

Bubble nucleation rate per unit time and per unit volume:

$$\Gamma(T) \sim T^4 e^{-\frac{S_3}{T}} \quad S_3 = \int d^3r \left[ \frac{1}{2} (\vec{\nabla} \varphi_b)^2 + V_{\text{eff}}(\varphi_b, T) \right]$$

$\varphi_b$ : Bounce solution



$$\begin{cases} \frac{d^2\varphi_b}{dr^2} + \frac{2}{r} \frac{d\varphi_b}{dr} - \frac{\partial V_{\text{eff}}}{\partial \varphi_b} = 0 \\ \frac{d\varphi_b}{dr} \Big|_{r=0} = 0, \quad \lim_{r \rightarrow \infty} \varphi_b = 0 \end{cases}$$

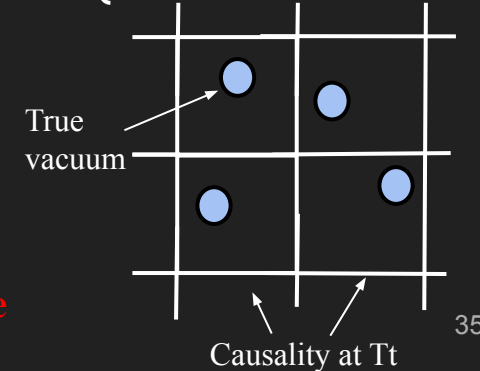
Transition temperature can be obtained by the following equation:

$$\Gamma / H^4 \Big|_{T=T_t} = 1 \longrightarrow$$

One bubble nucleates in the causality.

( $H$ : Hubble parameter)

**The transition temperature depends on the shape of the potential.**



# GW from first-order phase transition

- ★ The bubble dynamics is determined by the following parameters:

$$T_t, \alpha, \beta/H, v_b$$

**The GW spectrum from first-order EWPT can be featured these parameters.**

- (2)  $\alpha \sim$  Normalized latent heat released by EWPT

$$\alpha \equiv \frac{\epsilon(T_t)}{\rho_{\text{rad}}(T_t)}$$

$\epsilon$  : Latent heat     $\epsilon(T) = \Delta V_{\text{eff}}(T) - T \frac{\partial \Delta V_{\text{eff}}}{\partial T}$

$\rho_{\text{rad}}$  : Radiative energy density

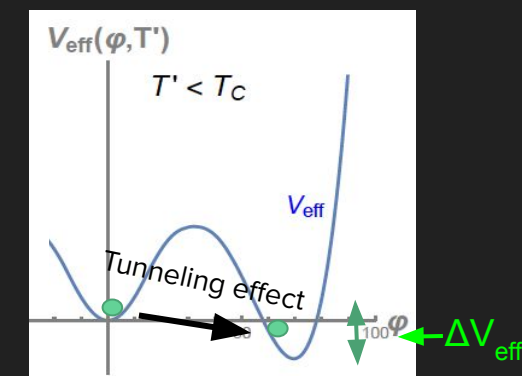
- (3)  $\beta/H \sim 1 / (\text{Duration of EWPT})$

$$\frac{\beta}{H_n} = T \frac{d(S_3(T)/T)}{dT} \Big|_{T=T_t}$$

$$\Gamma(T) \sim T^4 e^{-\frac{S_3}{T}}$$

- (4)  $v_b$  : Bubble wall velocity (It is related to the interaction between bubble and plasma.)

In this time, we treat it as constant.



# GW from first-order phase transition

- ★ Complicated numerical simulations are necessary to obtain the GW spectrum from first-order EWPT.

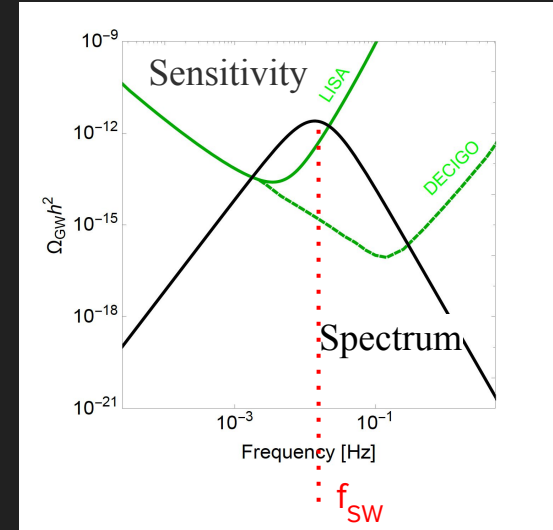
We use approximate fitting formula to evaluate it.

[M. Hindmarsh, S. J. Huber, K. Rummukainen and D. J. Weir, PRD 96, no.10, 103520 (2017)[erratum: PRD 101, no.8, 089902 (2020)], H. K. Guo, K. Sinha, D. Vagie and G. White, JHEP 06, 164 (2021)]

$$h^2\Omega_{\text{GW}}(f) = 8.5 \times 10^{-6} \left(\frac{100}{g_n}\right)^{1/3} \left(\frac{\kappa\alpha}{1+\alpha}\right)^2 \left(\frac{H_n}{\beta}\right) v_w S_{\text{SW}}(f)$$

$$S_{\text{SW}}(f) = \left(\frac{f}{f_{\text{SW}}}\right)^3 \left[\frac{7}{4+3(f/f_{\text{SW}})^2}\right]^{7/2} \quad f_{\text{SW}} = 1.9 \times 10^{-5} \frac{1}{v_w} \left(\frac{\beta}{H_n}\right) \left(\frac{T_n}{100 \text{ GeV}}\right) \left(\frac{g_n}{100}\right)^{1/6} \text{ Hz.}$$

$\kappa$  : efficiency factor



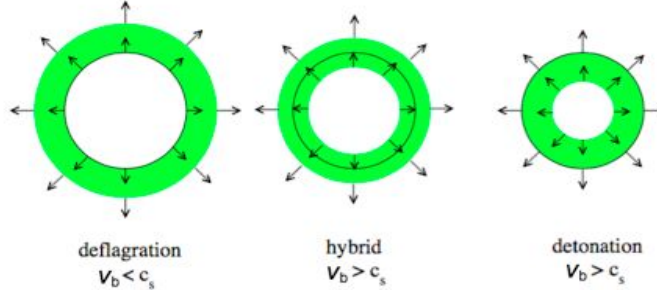
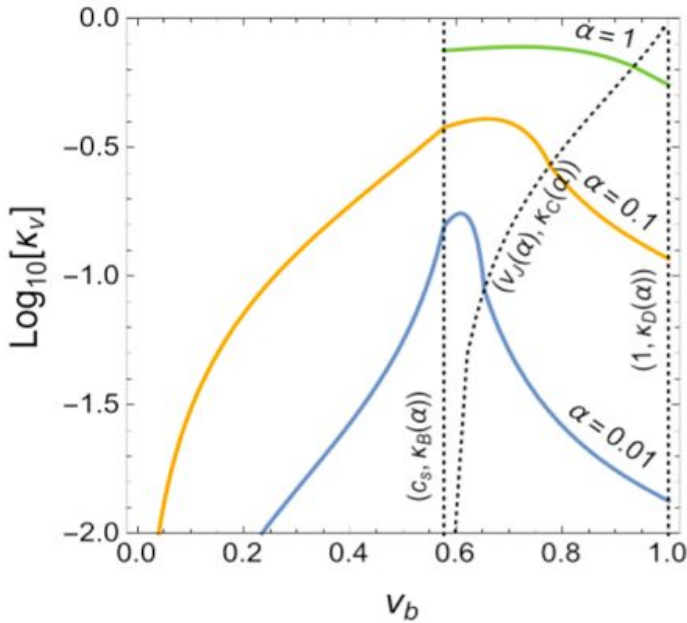
- ★ We use the signal to noise ratio to discuss whether the model can be tested by the GW observation.

$$\text{SNR} = \sqrt{\tau} \int_{f_{\min}}^{f_{\max}} df \left[ \frac{h^2\Omega_{\text{GW}}(f)}{h^2\Omega_{\text{Sens}}(f)} \right]^2 \quad (\text{T is the duration of experiments.})$$

When the ratio is larger than 10, we could typically detect the GW spectrum.

# Efficiency factors

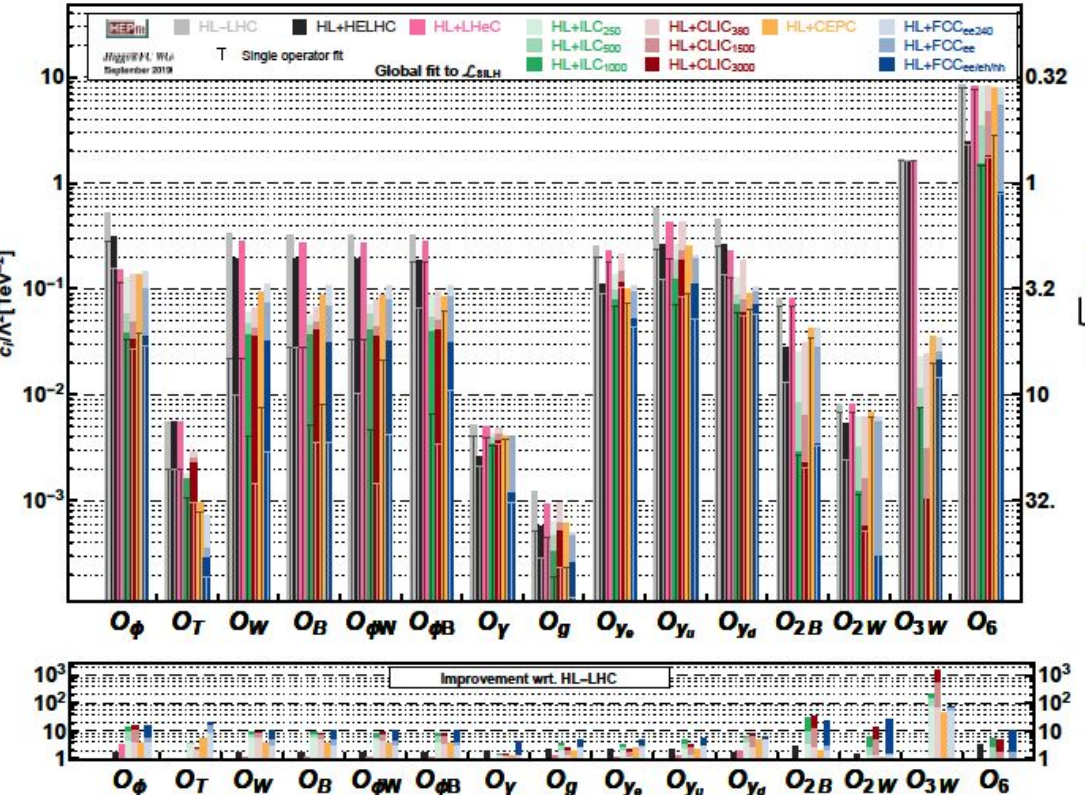
[J. R. Espinosa, T. Konstandin, J. M. No and G. Servant, JCAP 1006, 028 (2010)]



The black circle is bubble wall.  
In green we show the region of non-zero fluid velocity.

# EFT (dim. 6)

$1\sigma$

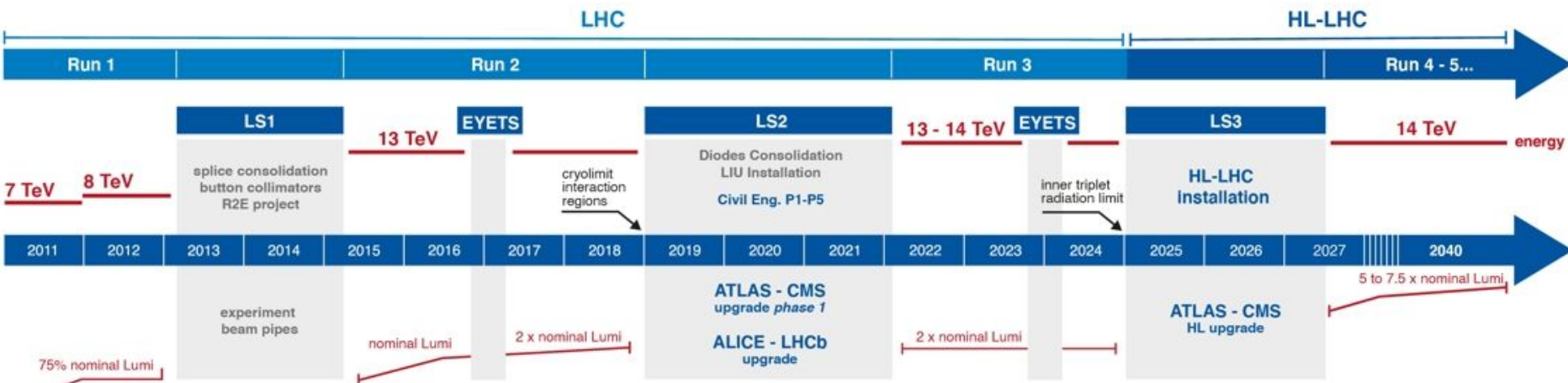


J. de Blas, M. Cepeda, J. D'Hondt, R. K. Ellis, C. Grojean, B. Heinemann, F. Maltoni, A. Nisati, E. Petit and R. Rattazzi, et al., JHEP 01 (2020), 139  
[arXiv:1905.03764 [hep-ph]].

$$\begin{aligned}
 \mathcal{L}_{\text{SILH}} = & \frac{c_\phi}{\Lambda^2} \frac{1}{2} \partial_\mu (\phi^\dagger \phi) \partial^\mu (\phi^\dagger \phi) + \frac{c_T}{\Lambda^2} \frac{1}{2} (\phi^\dagger \overset{\leftrightarrow}{D}_\mu \phi) (\phi^\dagger \overset{\leftrightarrow}{D}^\mu \phi) - \frac{c_6}{\Lambda^2} \lambda (\phi^\dagger \phi)^3 + \left( \frac{c_{y_f}}{\Lambda^2} y_f \right. \\
 & + \frac{c_W}{\Lambda^2} \frac{ig}{2} \left( \phi^\dagger \overset{\leftrightarrow}{D}_\mu \phi \right) D_\nu W^{a\mu\nu} + \frac{c_B}{\Lambda^2} \frac{ig'}{2} \left( \phi^\dagger \overset{\leftrightarrow}{D}_\mu \phi \right) \partial_\nu B^{\mu\nu} + \frac{c_{\phi W}}{\Lambda^2} ig D_\mu \phi^\dagger \sigma_a \\
 & \left. + \frac{c_\gamma}{\Lambda^2} g'^2 \phi^\dagger \phi B^{\mu\nu} B_{\mu\nu} + \frac{c_g}{\Lambda^2} g_s^2 \phi^\dagger \phi G^{A\mu\nu} G_{\mu\nu}^A \right. \\
 & \left. - \frac{c_{2W}}{\Lambda^2} \frac{g^2}{2} (D^\mu W_{\mu\nu}^a) (D_\rho W^{a\rho\nu}) - \frac{c_{2B}}{\Lambda^2} \frac{g'^2}{2} (\partial^\mu B_{\mu\nu}) (\partial_\rho B^{\rho\nu}) - \frac{c_{2G}}{\Lambda^2} \frac{g_S^2}{2} (D^\mu G_{\mu\nu}) (D_\rho G^{\rho\nu}) \right. \\
 & \left. + \frac{c_{3W}}{\Lambda^2} g^3 \epsilon_{abc} W_\mu^a W_\nu^b W_\rho^c \delta^{\mu\nu} + \frac{c_{3G}}{\Lambda^2} g_S^3 f_{ABC} G_\mu^A V G_V^B \rho G_\rho^C \mu \right),
 \end{aligned}$$



# LHC / HL-LHC Plan



## HL-LHC TECHNICAL EQUIPMENT:

DESIGN STUDY



PROTOTYPES

CONSTRUCTION

INSTALLATION & COMM.

PHYSICS

## HL-LHC CIVIL ENGINEERING:

DEFINITION

EXCAVATION

BUILDINGS

## ❖ Effective sensitivity

- LISA

$$S_{\text{eff}}(f) = \frac{20}{3} \frac{4S_{\text{acc}}(f) + S_{\text{sn}}(f) + S_{\text{omn}}(f)}{L^2} \left[ 1 + \left( \frac{f}{0.41c/2L} \right)^2 \right],$$

with  $L = 5 \times 10^9$  m and

$$\begin{aligned} S_{\text{acc}}(f) &= 9 \times 10^{-30} \frac{1}{(2\pi f/1\text{Hz})^4} \left( 1 + \frac{10^{-4}}{f/1\text{Hz}} \right) \text{ m}^2\text{Hz}^{-1}, \\ S_{\text{sn}}(f) &= 2.96 \times 10^{-23} \text{ m}^2\text{Hz}^{-1}, \\ S_{\text{omn}}(f) &= 2.65 \times 10^{-23} \text{ m}^2\text{Hz}^{-1}. \quad \text{“other measurement noise”} \end{aligned}$$

[A. Klein et al., Phys. Rev. D93 no. 2, (2016) 024003]

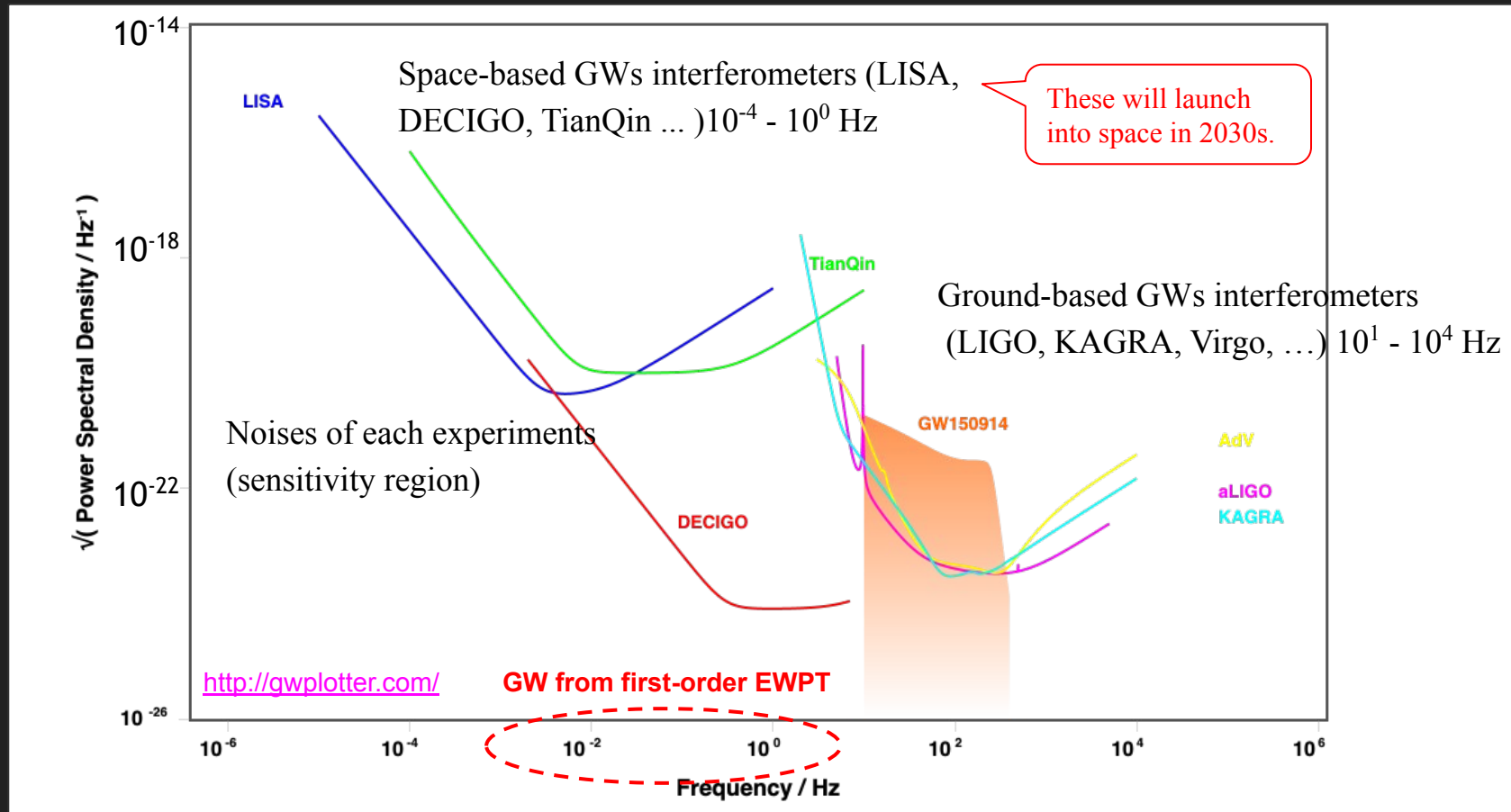
- DECIGO

$$\begin{aligned} S_{\text{eff}}(f) &= \left[ 7.05 \times 10^{-48} [1 + (f/f_p)^2] \right. \\ &\quad \left. + 4.8 \times 10^{-51} \frac{(f/1\text{Hz})^{-4}}{1 + (f/f_p)^2} + 5.33 \times 10^{-52} (f/1\text{Hz})^{-4} \right] \text{ Hz}^{-1}, \end{aligned}$$

with  $f_p = 7.36$  Hz.

[K. Yagi and N. Seto, Phys. Rev. D83 (2011) 044011]

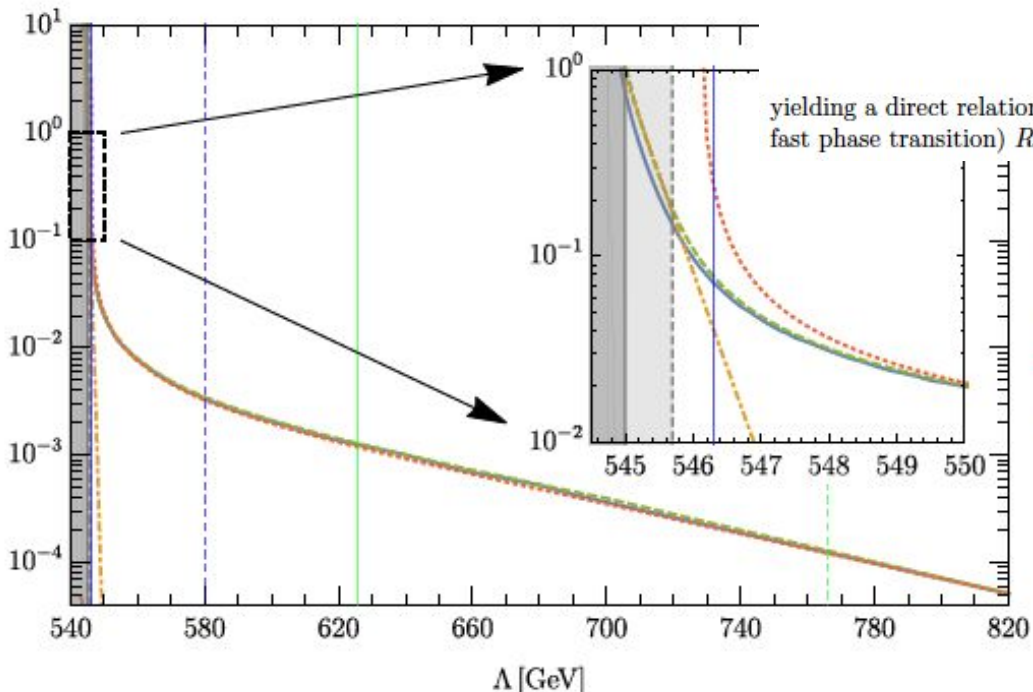
# GW interferometers



# About $HR_*$ (mean bubble separation)

$$\frac{1}{\mathcal{V}_{\text{false}}} \frac{d\mathcal{V}_{\text{false}}}{dt} = 3H(t) - \frac{dI(t)}{dt} = H(T) \left( 3 + T \frac{dI(T)}{dT} \right) < 0$$

J. Ellis, M. Lewicki and J. M. No, JCAP 04 (2019), 003,  
[\[arXiv:1809.08242 \[hep-ph\]\]](https://arxiv.org/abs/1809.08242)



The mean bubble separation

yielding a direct relation between  $\beta$  and the mean bubble centre separation (in the case of a fast phase transition)  $R_{*R}$ . This relation is approximately maintained at  $T = T_p$ .

$$n_B = (R_{*R})^{-3} = \frac{1}{8\pi} \left( \frac{\beta}{v_w} \right)^3, \quad (3.4)$$

$HR_{\text{MAX}}$  (Strong phase transition)  
 $HR_*$   
 $HR_{*R}$

$$n_B = (R_{*V})^{-3} \simeq \sqrt{2\pi} \frac{\Gamma(T_m)}{\beta_V}$$

$HR_{*V}$  (General case)

$$n_B = (R_*)^{-3} = \int_{t_c}^t dt' \frac{a(t')^3}{a(t)^3} \Gamma(t') P(t')$$

$$\text{Energy distribution: } \mathcal{E}_B(t, R) \equiv R^3 \frac{dn}{dR}(t, R)$$

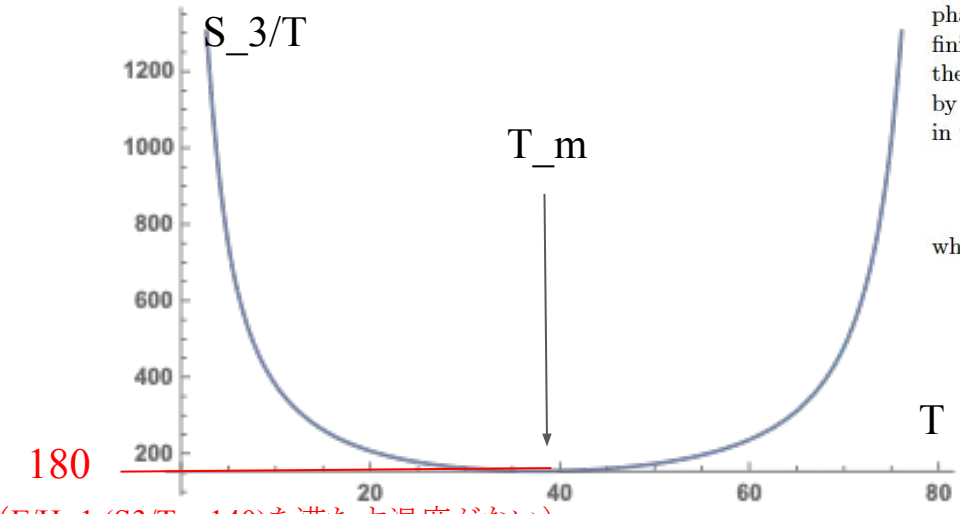
Since the energy budget of a bubble scales with its volume  $R^3$ .

relevant for GW generation:  $R_{\text{MAX}}$  (solid blue), the size of the bubbles carrying the largest fraction of energy on completion of the transition, and  $R_*$  (dashed green), the mean bubble separation. We also show the approximation to the latter assuming radiation domination  $R_{*R}$  (3.4) (dashed red) and vacuum domination  $R_{*V}$  (3.7) (dash-dot yellow). We see that

# About $\beta$

$$\Gamma \propto e^{-\frac{S_3(T)}{T}} = e^{\beta(t-t_0) + \dots}$$

## ★ 線形近似が使えない場合



相転移が低温度の場合(例えば  $\Gamma/H=1$  の条件を満たせないような時)、  
 $\Gamma$  の Linear approximation が break down する可能性がある

➡ その時は Next order に注目する

J. Ellis, M. Lewicki and J. M. No, JCAP 04 (2019), 003,  
[arXiv:1809.08242 [hep-ph]]

For very strong phase transitions, a potential barrier between the symmetric and broken phases may still be present at  $T = 0$ , which results in  $S_3(T)/T$  having a minimum at some finite  $T$ . The linear approximation (3.2) may then break down [45, 79] (see also [80]), as the first derivative of the bounce action can vanish (the timescale of the transition defined by (3.3) then yields  $\beta_R \rightarrow 0$  and even turns negative). In this case, going to the next order in the Taylor expansion of the bounce action, we obtain a Gaussian approximation

$$\Gamma \propto e^{-\frac{S_3(T)}{T}} = e^{-\frac{1}{2}\beta_V^2(t-t_m)^2 + \dots}, \quad (3.5)$$

where  $t_m$  corresponds to  $(d/dt)(S_3(T)/T)|_{t=t_m} = 0$ , and  $\beta_V$  is given by

$$\beta_V \equiv \sqrt{\left. \frac{d^2}{dt^2} \left( \frac{S_3(T)}{T} \right) \right|_{t=t_m}} = H(T)T \sqrt{\left. \frac{d^2}{dT^2} \left( \frac{S_3(T)}{T} \right) \right|_{T=T_m}}. \quad (3.6)$$

$$\Gamma \propto e^{-\frac{S_3(T)}{T}} = e^{\beta(t-t_0) + \dots}$$



$$\Gamma \propto e^{-\frac{S_3(T)}{T}} = e^{-\frac{1}{2}\beta_V^2(t-t_m)^2 + \dots}$$

$$\Gamma(T) \simeq \max \left[ T^4 \left( \frac{S_3}{2\pi T} \right)^{\frac{3}{2}} \exp(-S_3/T), R_0^{-4} \left( \frac{S_4}{2\pi} \right)^2 \exp(-S_4) \right]$$

# About T\_p

相転移の温度が高い場合  $T_n \sim T_p$

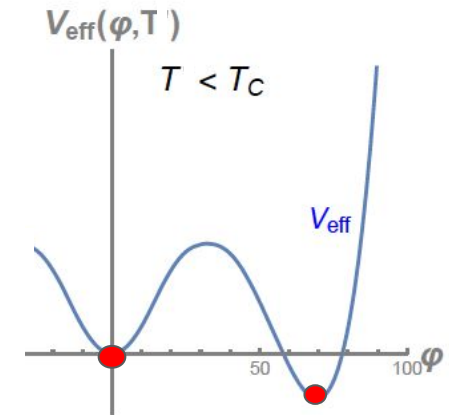
$T_p$ とは  $P(T)=0.34$ となるときの温度 ( $P(T)$ は False vacuum space が空間にどれだけ占められているのかを表す) であり、相転移が完了したときの温度に対応する

## ★ How to evaluate $T_p$ by “Mathematica” ?

1. Fixing benchmark point including temperature
2. Evaluating minima points (Red points)
3. Obtaining  $S_3$  and  $S_4$
4. Comparing  $T^4 \left( \frac{S_3}{2\pi T} \right)^{\frac{3}{2}} \exp(-S_3/T)$ ,  $R_0^{-4} \left( \frac{S_4}{2\pi} \right)^2 \exp(-S_4)$
5. Integrating  $I(T) = \frac{4\pi}{3} \int_T^{T_c} \frac{dT' \Gamma(T')}{H_V T'^4 \sqrt{1 + \chi(T')^{-1}}} \left( \int_T^{T'} \frac{d\tilde{T}}{H_V \sqrt{1 + \chi(\tilde{T})^{-1}}} \right)^3$
6. A condition of percolation temperature  $I(T_p) = 0.34$



$$\frac{1}{V_{\text{false}}} \frac{dV_{\text{false}}}{dt} = 3H(t) - \frac{dI(t)}{dt} = H(T) \left( 3 + T \frac{dI(T)}{dT} \right) < 0$$



$$P(t) = e^{-I(t)}, \quad I(t) = \frac{4\pi}{3} \int_{t_c}^t dt' \Gamma(t') a(t')^3 r(t, t')^3$$

<sup>4</sup>Some early works in the context of cosmological first-order phase transitions [78] defined the onset of bubble coalescence as  $P(t_0) = 1/e \rightarrow I(t_0) = 1$ , yielding a slightly lower percolation temperature.